Eur. Phys. J. C 18, 731–746 (2001)
Digital Object Identifier (DOI) 10.1007/s100520100583

THE EUROPEAN
PHYSICAL JOURNAL C

Charge asymmetry of pions in the process $e^-e^+ \to e^-e^+\pi^+\pi^-$

I.F. Ginzburg[1,2,a], A. Schiller[3,b], V.G. Serbo[2,c]

[1] Sobolev Institute of Mathematics, 630090 Novosibirsk, Russia
[2] Novosibirsk State University, 630090 Novosibirsk, Russia
[3] Institut für Theoretische Physik and NTZ, Universität Leipzig, 04109 Leipzig, Germany

Received: 6 December 2000 / Published online: 5 February 2001 – © Springer-Verlag 2001

Abstract. The study of the charge asymmetry of produced particles allows one to investigate the interference of different production mechanisms and to determine new features of the corresponding amplitudes. In the process $e^-e^+ \to e^-e^+\pi^+\pi^-$ the two-pion system is produced via two mechanisms: two-photon (C-even state) and bremsstrahlung (C-odd state) production. We study the charge asymmetry of pions differentially in the pion momenta cross section originating from interference between these two mechanisms. At low effective mass of the dipions this asymmetry is directly related to the s- and p-phases of elastic $\pi\pi$ scattering. At higher energies it can give new information about the f_0 meson family, the $f_2(1270)$ meson, etc. The asymmetry is expressed via the pion form factor F_π and the helicity amplitudes M_{ab} for the subprocess $\gamma^*\gamma \to \pi^+\pi^-$ as $\sum G_{ab}\mathrm{Re}(F_\pi^* M_{ab})$, where we have analytically calculated the coefficients G_{ab} for the region giving the main contribution to the effect. Several distributions of the pions are presented performing a numerical analysis in a model with point-like pions. In the region near the dipion threshold the asymmetry is of the order of 1%. We show that with suitable cuts the signal to background ratio can be increased up to about 10%.

1 Introduction

The study of charge asymmetry in particle production can be used as an essential source of information about production amplitudes which is difficult to obtain otherwise. In this paper we discuss the charge asymmetry of pions produced in the reaction $e^-e^+ \to e^-e^+\pi^+\pi^-$. The pion pair (dipion) in this process is produced mainly via the two-photon mechanism (Fig. 1) or via bremsstrahlung (Fig. 2).

The first of them gives charge parity even (C-even) dipions, while the second mechanism leads to C-odd pion pairs. In the differential cross section the interference of these mechanisms results in terms which are antisymmetric under $\pi^+ \leftrightarrow \pi^-$ exchange. Certainly, these terms disappear in the total cross section or after a suitable averaging. Nevertheless, they are observable and could give new information about the production amplitudes which cannot be obtained unambiguously by other approaches. In particular, at low effective masses of the dipions $W \sim 2m_\pi$ this interference is directly related to the difference of s- and p-phase shifts of the elastic $\pi\pi$ scattering. These phase shifts are of primary importance for low energy hadron physics [1,2] (in particular, for the chiral dynamics which pretends to be the low energy version of QCD). At higher energies the interference can give new information about the $f_0(400\text{–}1200)$ meson (former σ), the $f_0(980)$ meson, etc. The nature of these particles presently is widely discussed.

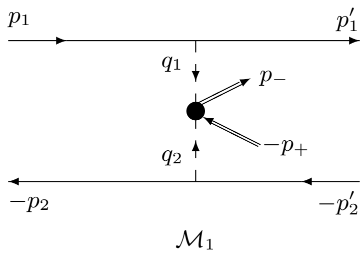

Fig. 1. Amplitude $\mathcal{M}_1$ for the two-photon production of pions. The e^- and e^+ with initial 4-momenta (energies) p_1 (E_1) and p_2 (E_2) and final momenta (energies) p_1' (E_1') and p_2' (E_2') emit virtual photons with $q_i = p_i - p_i'$ ($\omega_i = E_i - E_i'$). These photons produce the C-even $\pi^+\pi^-$ system with total 4-momentum $k = p_+ + p_- = q_1 + q_2$ and effective mass $W = \sqrt{k^2}$; furthermore $s = (p_1 + p_2)^2 = 4E_1E_2$

The opportunity of using C-odd effects for such problems was first studied almost three decades ago in [3]. In that paper the case of the small total transverse momenta of the produced pion pair, $\mathbf{k}_\perp^2 \ll m_\pi^2$, was considered. However, this region gives only a small fraction of the entire charge asymmetry discussed. In this paper we obtain formulae which allow one to study the charge asymmetry

[a] e-mail: ginzburg@math.nsc.ru
[b] e-mail: Arwed.Schiller@itp.uni-leipzig.de
[c] e-mail: serbo@math.nsc.ru

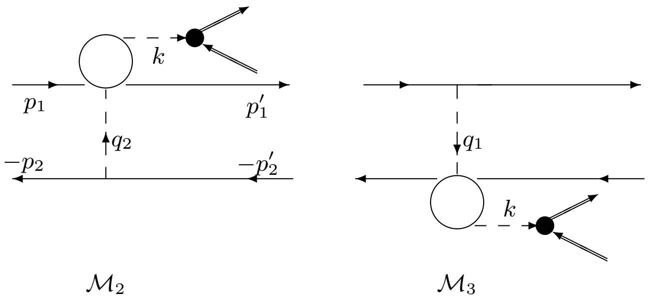

Fig. 2. Amplitudes $\mathcal{M}_2$ and $\mathcal{M}_3$ for the bremsstrahlung production of pions. The pion pair in the C-odd state is produced by one virtual photon with 4-momentum $k = p_+ + p_-$ emitted by the electron ($\mathcal{M}_2$) or by the positron ($\mathcal{M}_3$). The open circles represent the virtual Compton scattering shown in Fig. 3

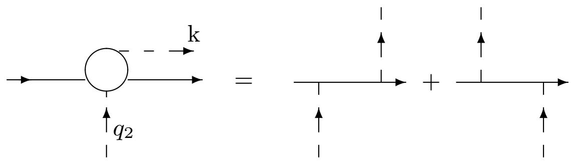

Fig. 3. Virtual Compton scattering

in the main kinematical region, $k_\perp \lesssim W$, and discuss the main features of the effect and the background.

Recently the process $e^+e^- \to e^+e^-\pi^+\pi^-$ was considered in [4] for the case when the virtuality of one photon is large, $-q_1^2 \gg W^2$. The authors concentrate their efforts on a QCD analysis of the exclusive dipion production in a $\gamma^*\gamma$ collision in that region (leading to a factorization of perturbative QCD subprocesses and a generalized two-meson distribution amplitude). The developed description of the process at e^+e^- colliders also includes the interference of two-photon and bremsstrahlung production mechanisms. Naturally, the estimates for the possible number of events of that work are considerably lower than those in the main region considered in the present paper. Note that the discussed charge asymmetry was observed at CLEO in the $e^+e^- \to e^+e^-\pi\pi$ reaction detecting additionally an electron scattered at large angle [5][1].

The effect of interest can be studied on e^+e^- colliders with c.m. energies above 1 GeV. We show that the charge asymmetry is of the order of 1% and that the signal to background ratio can be considerably improved with suitable cuts. Let us emphasize that in the method of data preparation suggested in the present paper, the considered asymmetries can be obtained from the data independent on the uncertainty in calculating the background.

We consider an experimental set-up when only pion momenta $\mathbf{p}_+$ and $\mathbf{p}_-$ are measured (the so-called *no tag* experiments). This set-up corresponds to the cross section $\mathrm{d}\sigma/(\mathrm{d}^3p_+\mathrm{d}^3p_-)$ for the $e^-e^+ \to e^-e^+\pi^+\pi^-$ process. Besides, our results are also valid for the *single tag* experiments in which additionally the scattered electron is recorded, and where an averaging is performed over the small unbalance of transverse momentum of the scattered electron and the dipion.

The outline of our paper is as follows: First we present a qualitative description of different contributions to the reaction $e^-e^+ \to e^-e^+\pi^+\pi^-$. In Sect. 3 the necessary variables are defined and the basic formulae are presented. The amplitude of the subprocess $\gamma^*\gamma^* \to \pi^+\pi^-$ is represented via helicity amplitudes in a model independent way. The charge asymmetry of pions is calculated in Sect. 4. The obtained result [see (28), (29) and (31)] is given in a simple analytical form. To discuss the background problems more accurately, we present in Sect. 5 approximate formulae for the two-photon and bremsstrahlung production in the kinematical region which is essential for the charge asymmetry. In Sect. 6 we present an approximate description of the $\gamma^*\gamma \to \pi^+\pi^-$ subprocess entering the two-photon amplitude. To get an idea about the potentiality of future experiments we perform a numerical analysis in Sect. 7 restricting ourselves to the QED model (point-like pions) for the amplitudes which gives a reasonable description at $W < 1$ GeV. We present several important distributions and estimate the background. Additionally we study the charge asymmetry of muons in the process $e^+e^- \to e^+e^-\mu^+\mu^-$ (Sect. 8). In the final section we summarize our results. Details of the calculations are presented in the Appendices.

2 Qualitative description of different contributions

The main contribution to the cross section of the process can be written via the amplitudes $\mathcal{M}_j$ shown in Figs. 1 and 2. It is a sum of C-even, C-odd and interference contributions:

$$\mathrm{d}\sigma = \mathrm{d}\sigma_{C=+1} + \mathrm{d}\sigma_{C=-1} + \mathrm{d}\sigma_{\mathrm{interf}}, \qquad (1)$$

where

$$\begin{aligned}
&\mathrm{d}\sigma_{C=+1} \propto |\mathcal{M}_1|^2,\\
&\mathrm{d}\sigma_{C=-1} = \mathrm{d}\sigma_2 + \mathrm{d}\sigma_3 \propto |\mathcal{M}_2|^2 + |\mathcal{M}_3|^2,\\
&\mathrm{d}\sigma_{\mathrm{interf}} = \mathrm{d}\sigma_{12} + \mathrm{d}\sigma_{13},\\
&\mathrm{d}\sigma_{12} \propto 2\mathrm{Re}(\mathcal{M}_2^*\mathcal{M}_1), \quad \mathrm{d}\sigma_{13} \propto 2\mathrm{Re}(\mathcal{M}_3^*\mathcal{M}_1).
\end{aligned} \qquad (2)$$

Let us discuss these contributions qualitatively. In the head-on collisions of the leptons the z-axis is chosen along the initial electron momentum.

[1] A similar problem was discussed in [6] for ep scattering related to HERA experiments. Unfortunately, those results have no direct relation to experiments since the main C-odd contribution in ep scattering is given by the production of ρ mesons via strong interactions (diffractive production for pions flying along electrons or proton excitation for pions flying along protons). The bremsstrahlung production considered in [6] is suppressed roughly by a factor $\alpha = 1/137$. Besides, the authors of [6] claim that their formulae (obtained for $ep \to ep\pi^+\pi^-$) are valid for the pion charge asymmetry in the process $e^-e^+ \to e^-e^+\pi^+\pi^-$. In that respect their results are definitely incorrect since contributions of zero helicity for the virtual photon are not included. As we show here, these contributions are of the same order of magnitude as those with helicity ±1 (see Sect. 4 for details)

The two-photon mechanism (Fig. 1) produces C-even dipions. It provides the main contribution to the total cross section. The corresponding part of the cross section $\mathrm{d}\sigma_{C=+1}$ can be expressed via the amplitudes M_{ab} describing the collisions of virtual photons with helicities a and b $(a, b = \pm 1, 0)$ [7]. Its dominant part is given by almost real photons which have virtualities q_1^2 and q_2^2 close to zero (small transfer momenta squared of electrons and positrons). The produced pairs are distributed almost uniformly over their total rapidity and peaked at small values of their total transverse momentum $k_\perp$ (for details see the review of [8]). In this kinematical region only the transverse helicities $(a, b = \pm 1)$ for almost on-shell photons give the dominant contribution and the cross section can be written via $|M_{++}|^2$, $|M_{+-}|^2$ and $\mathrm{Re}(M_{+-}^* M_{++})$.

The bremsstrahlung mechanism (Fig. 2) produces pion pairs in the C-odd state. Its contribution to the cross section $\mathrm{d}\sigma_{C=-1}/(\mathrm{d}^3p_+\mathrm{d}^3p_-)$ was calculated in [9]. It is proportional to $|F_\pi(k^2)|^2$ where F_π is the pion form factor. The main contribution to $\mathrm{d}\sigma_2$ is given by the region where the exchange photon with momentum q_2 is almost real. In that domain the sum of energy and longitudinal momentum of the produced pair is close to that of the initial electron, while the transverse momentum of the pair $k_\perp$ is very small.

However, in the kinematical region essential for both two-photon production and interference, the $k_\perp$-distribution of the pions is relatively wide. The interference between bremsstrahlung by an electron (amplitude $\mathcal{M}_2$) and by a positron ($\mathcal{M}_3$) is negligible small. Note that both contributions $\mathrm{d}\sigma_{C=+1}$ and $\mathrm{d}\sigma_{C=-1}$ are charge symmetric; they do not change under pion exchange $\pi^+ \leftrightarrow \pi^-$.

The interference of C-even and C-odd contributions $\mathrm{d}\sigma_{\mathrm{interf}} = \mathrm{d}\sigma_{12} + \mathrm{d}\sigma_{13}$ [see (2)] is antisymmetric under pion exchange, $\pi^+ \leftrightarrow \pi^-$, due to opposite charge parities of the dipion states produced by two-photon and bremsstrahlung mechanisms. Therefore, this interference determines *the charge asymmetry of pions*, i.e.

$$\mathrm{d}\sigma_{\mathrm{interf}} = \frac{1}{2}\left[\mathrm{d}\sigma(p_+, p_-, \ldots) - \mathrm{d}\sigma(p_-, p_+, \ldots)\right]. \tag{3}$$

To discuss this asymmetry, it is useful to introduce the operator of charge conjugation of pions $\hat{C}_\pi$ by its action on an arbitrary function $F(p_+, p_-)$:

$$\hat{C}_\pi F(p_+, p_-) = F(p_-, p_+). \tag{4}$$

In particular, we have

$$\hat{C}_\pi \mathrm{d}\sigma_{C=\pm 1} = \mathrm{d}\sigma_{C=\pm 1}, \quad \hat{C}_\pi \mathrm{d}\sigma_{\mathrm{interf}} = -\mathrm{d}\sigma_{\mathrm{interf}}.$$

Many features of this interference can naturally be explained taking into account the described features of the two-photon and bremsstrahlung production. For example, the main contribution to $\mathrm{d}\sigma_{12}$ is given by an almost real photon q_2 (small transfer momentum squared of the positron). The produced pions fly mainly along the electron, $k_z = p_{+z} + p_{-z} > 0$, and the dipion transverse momentum distribution is not peaked at small $k_\perp$. Therefore the transverse momentum of the electron is not small, $\mathbf{q}_{1\perp} \approx \mathbf{k}_\perp$. Similarly, the main contribution to $\mathrm{d}\sigma_{13}$ is given by the almost real photon q_1 (small transfer momentum squared of the electron), whereas the transverse momentum of the positron is not small, $\mathbf{q}_{2\perp} \approx \mathbf{k}_\perp$. The produced pions fly mainly along the positron, $k_z < 0$.

Certainly, the sign of the observed effect is different for $\mathrm{d}\sigma_{12}$ (related to bremsstrahlung production of pions by an electron with negative charge) and for $\mathrm{d}\sigma_{13}$ (related to bremsstrahlung production of pions by an positron with positive charge). Therefore, some details of the asymmetry are different for e^+e^- and e^-e^- collisions.

Let us first consider the *s-channel contributions*. In the previous discussion we did not consider the additional set of diagrams which can be obtained from those in Figs. 1 and 2 interchanging the outgoing electron by the incoming positron ($p_1' \leftrightarrow -p_2$), etc. The contributions of those diagrams contain an additional factor $1/s$ due to the photon propagator. Besides, the final electron and positron have a wide angular distribution in the main regions and, therefore, do not give a logarithmic enhancement (contrary to the considered diagrams). As a result, the contributions of the s-channel (annihilation) diagrams and their interference with those of Figs. 1 and 2 are suppressed by a factor $W^2/(sL)$ where $L \sim 10 \div 15$ is a typical logarithm.

3 Basic notations and general formulae

Our main notational conventions are given in Figs. 1 and 2. As already mentioned, we consider the head-on collisions of electrons and positrons with the z-axis along the initial electron momentum. In this frame $p_i = (E_i, 0, 0, \pm(E_i^2 - m_e^2)^{1/2})$, $i = 1, 2$. The virtual photon momenta for the two-photon production of Fig. 1 are $q_i = p_i - p_i' = (\omega_i, \mathbf{q}_{i\perp}, q_{iz})$ with

$$q_i^2 = 2q_ip_i = -\frac{\mathbf{q}_{i\perp}^2 + m_e^2(\omega_i/E_i)^2}{1 - (\omega_i/E_i)} < 0. \tag{5}$$

The 4-momenta of the produced pions are given by $p_\pm = (\varepsilon_\pm, \mathbf{p}_{\pm\perp}, p_{\pm z})$ with $p_\pm^2 = \mu^2$. Below we use the quantities

$$x_\pm = \frac{\varepsilon_\pm + p_{\pm z}}{2E_1} = \frac{p_\pm p_2}{p_1 p_2}, \quad y_\pm = \frac{\varepsilon_\pm - p_{\pm z}}{2E_2} = \frac{p_\pm p_1}{p_2 p_1},$$
$$x = x_+ + x_-, \quad y = y_+ + y_-. \tag{6}$$

For ultra-relativistic pions flying along the initial electron or positron momentum, the quantity $x_\pm$ $(y_\pm)$ is the fraction of energy transferred from the electron (positron) to $\pi^\pm$. The variables $x_\pm$ $(y_\pm)$ appear in the cross section $\mathrm{d}\sigma_{12}$ $(\mathrm{d}\sigma_{13})$.

In what follows, we consider the symmetric and antisymmetric combinations of the pion momenta:

$$k = p_+ + p_-, \qquad \varDelta = p_+ - p_-. \tag{7}$$

The pion charge conjugation operator leads in particular to

$$\hat{C}_\pi \varDelta^\mu = -\varDelta^\mu.$$

Therefore, the asymmetry effects are proportional to the components of the 4-vector $\varDelta$.

To describe that asymmetry we use the variables

$$\begin{aligned} \xi &= \frac{x_+ - x_-}{x} = \frac{p_2\Delta}{p_2 k}, \\ \eta &= \frac{y_+ - y_-}{y} = \frac{p_1\Delta}{p_1 k}, \\ K_- &= \frac{(p_2-p_1)\Delta}{(p_2+p_1)k} = \frac{x\xi - y\eta}{x+y}, \\ v &= \mathbf{p}_{+\perp}^2 - \mathbf{p}_{-\perp}^2 = \mathbf{k}_\perp \boldsymbol{\Delta}_\perp. \end{aligned} \tag{8}$$

The "transverse" variable v is a natural variable both for contributions $\mathrm{d}\sigma_{12}$ and $\mathrm{d}\sigma_{13}$. The "longitudinal" variable ξ naturally arises in describing the contribution $\mathrm{d}\sigma_{12}$ (whereas η arises in describing $\mathrm{d}\sigma_{13}$). The symmetric variable K_- is suitable to discuss the sum $\mathrm{d}\sigma_{12} + \mathrm{d}\sigma_{13}$. Note that K_- is proportional to the difference of the longitudinal momenta of π^+ and π^- in the e^-e^+ center-of-mass system

$$K_- = \left\{ \frac{p_{+z} - p_{-z}}{\varepsilon_+ + \varepsilon_-} \right\}_{e^-e^+\text{c.m.s.}}.$$

Besides, $K_- = \xi$ at $x \gg y$ and $K_- = -\eta$ at $x \ll y$.

The amplitude $\mathcal{M}_1$ *of the two-photon production* is written via the amplitude $M^{\mu\nu}$ of the subprocess $\gamma^*\gamma^* \to \pi^+\pi^-$ as

$$\mathcal{M}_1 = \frac{4\pi\alpha}{q_1^2 q_2^2} \left(\bar{u}_1' \gamma_\mu u_1\right) \left(\bar{v}_2 \gamma_\nu v_2'\right) M^{\mu\nu}, \tag{9}$$

where the bispinors $u_1(u_1')$ and $v_2(v_2')$ correspond to the initial (final) electron and positron, respectively.

Instead of the amplitude $M^{\mu\nu}$ it is more convenient to use the helicity amplitudes M_{ab} which can be introduced via[2]

$$M_{\mu\nu} = \sum_{ab=\pm1,0} (-1)^{a+b} e_{1\mu}^{(a)*} e_{2\nu}^{(b)*} M_{ab}. \tag{10}$$

Here $e_{j\mu}^{(a)}$ is the polarization vector of the jth virtual photon with helicity $a = \pm1, 0$. A virtual photon is called *transverse* if its helicity is equal to ±1 and *scalar (longitudinal)* for zero helicity. Since the amplitude $M^{\mu\nu}$ is C-even, the vectors of transverse and scalar polarization are C-odd and C-even, respectively (see Appendix A for details):

$$\begin{gathered} \hat{C}_\pi M^{\mu\nu} = M^{\mu\nu}, \\ \hat{C}_\pi e_{i\mu}^{(\pm1)} = -e_{i\mu}^{(\pm1)}, \qquad \hat{C}_\pi e_{i\mu}^{(0)} = e_{i\mu}^{(0)}, \end{gathered} \tag{11}$$

and we get

$$\hat{C}_\pi M_{0\pm} = -M_{0\pm}, \quad \hat{C}_\pi M_{+\pm} = M_{+\pm}. \tag{12}$$

It is important that the amplitudes M_{ab} with scalar photons disappear near the photon mass shell:

$$\begin{gathered} M_{0\pm} \propto \sqrt{-q_1^2}, \quad M_{\pm0} \propto \sqrt{-q_2^2}, \quad M_{00} \propto \sqrt{q_1^2 q_2^2}, \\ \text{at } q_{1,2}^2 \to 0. \end{gathered} \tag{13}$$

[2] Details of kinematics for the subprocess $\gamma^*\gamma^* \to \pi^+\pi^-$ are given in Appendix A

So the amplitude $\mathcal{M}_1$ of the two-photon production can be represented in the form

$$\begin{aligned} \mathcal{M}_1 = \frac{4\pi\alpha}{q_1^2 q_2^2} & \sum_{ab=\pm1,0} (-1)^{a+b} \\ & \times \left(\bar{u}_1' \hat{e}_1^{(a)*} u_1\right) \left(\bar{v}_2 \hat{e}_2^{(b)*} v_2'\right) M_{ab}. \end{aligned} \tag{14}$$

In a similar way *the amplitude* $\mathcal{M}_2$ *of the bremsstrahlung production* by an electron can be written as

$$\begin{aligned} \mathcal{M}_2 &= \frac{(4\pi\alpha)^2}{q_2^2 k^2} F_\pi(k^2) \\ &\quad \times \sum_{c=\pm1,0} (-1)^c \left(\bar{u}_1' \hat{C}^{(c)} u_1\right) \left(\bar{v}_2 \hat{e}_2^{(c)*} v_2'\right), \\ \hat{C}^{(c)} &= \hat{\Delta} \frac{\hat{p}_1' + \hat{k} + m_e}{(p_1'+k)^2 - m_e^2} \hat{e}_2^{(c)} + \hat{e}_2^{(c)} \frac{\hat{p}_1 - \hat{k} + m_e}{(p_1 - k)^2 - m_e^2} \hat{\Delta}, \end{aligned} \tag{15}$$

where the quantity $\bar{u}_1' \hat{C}^{(c)} u_1$ corresponds to the amplitude of the virtual Compton scattering shown in Fig. 3; $F_\pi(k^2)$ is the pion form factor.

As a result, *the interference of the amplitudes of* $\mathcal{M}_1$ *and* $\mathcal{M}_2$ is given by the expression

$$\begin{aligned} \mathrm{d}\sigma_{12} &= 2\mathrm{Re}(\mathcal{M}_2^* \mathcal{M}_1) \frac{\mathrm{d}\Gamma}{2s} \\ &= -2 \frac{(4\pi\alpha)^3}{q_1^2 q_2^2 k^2} \sum_{abc=\pm1,0} \mathrm{Re}\left(F_\pi^* M_{ab} \varrho_2^{bc} C_1^{ac}\right) \frac{\mathrm{d}\Gamma}{2s}, \end{aligned} \tag{16}$$

where the phase volume of the final particles is

$$\begin{aligned} \mathrm{d}\Gamma &= (2\pi)^4 \delta(p_1 + p_2 - p_1' - p_2' - p_+ - p_-) \\ &\quad \times \frac{\mathrm{d}^3 p_1' \mathrm{d}^3 p_2'}{2E_1' 2E_2' (2\pi)^6} \frac{\mathrm{d}^3 p_+ \mathrm{d}^3 p_-}{2\varepsilon_+ 2\varepsilon_- (2\pi)^6}, \end{aligned} \tag{17}$$

the (non-normalized) density matrix of the second virtual photon is

$$\rho_2^{bc} = \frac{(-1)^{b+c}}{2(-q_2^2)} \mathrm{Tr}\left\{(\hat{p}_2 - m_e)\hat{e}_2^{(b)*}(\hat{p}_2' - m_e)\hat{e}_2^{(c)}\right\} \tag{18}$$

and

$$C_1^{ac} = \frac{(-1)^a}{2} \mathrm{Tr}\left\{(\hat{p}_1' + m_e)\hat{e}_1^{(a)*}(\hat{p}_1 + m_e)\hat{C}^{(c)*}\right\}. \tag{19}$$

4 The charge asymmetry

Let us remind the reader that the charge asymmetry is determined by the two contributions $\mathrm{d}\sigma_{12}$ and $\mathrm{d}\sigma_{13}$ arising from the interference of the two-photon diagram of Fig. 1 with bremsstrahlung diagrams of Fig. 2, [see (2)]. Calculating this asymmetry we limit ourselves to logarithmic accuracy (which is about 5% in our case).

First, we discuss *the contribution* $\mathrm{d}\sigma_{12}$. According to the qualitative description in Sect. 2 the main contribution to $\mathrm{d}\sigma_{12}$ is given by very small values of $(-q_2^2)$. Therefore, the second virtual photon can be considered as almost real. Taking into account (5) we can use in all expressions

$$q_2^2 = 0, \quad \mathbf{q}_{2\perp} = 0, \quad \mathbf{q}_{1\perp} = \mathbf{k}_\perp, \quad q_1^2 = -\frac{\mathbf{k}_\perp^2}{1-x}, \tag{20}$$

except for the propagator of the second photon in the matrix element $\mathcal{M}_1$ [see (9) and (14)]. This has the consequence that in this limit the amplitudes M_{ab} with $b = 0$ can be safely neglected [see (13)].

To obtain $\mathrm{d}\sigma_{12}/(\mathrm{d}^3p_+\mathrm{d}^3p_-)$, we transform the phase volume (17) to the form

$$\mathrm{d}\Gamma = \frac{\mathrm{d}^2 q_{2\perp}}{32(2\pi)^8(E_1-\omega_1)(E_2-\omega_2)}\frac{\mathrm{d}^3p_+\mathrm{d}^3p_-}{\varepsilon_+\varepsilon_-} \tag{21}$$

and integrate either over $\mathbf{q}_{2\perp}$ or q_2^2 and φ_2. The latter is the azimuthal angle of the vector $\mathbf{q}_{2\perp}$. After integrating over φ_2 the non-diagonal elements of the ρ_2^{bc} matrix disappear and the final result contains $\rho_2^{++} = \rho_2^{-}$ only (i.e. $b = c = \pm 1$)

$$\int \rho_2^{bc}\frac{\mathrm{d}|q_2^2|}{|q_2^2|}\mathrm{d}\varphi_2 = 2\pi\delta_{bc}\rho_2^{++}L_2,$$

$$L_2 = \int \frac{\mathrm{d}|q_2^2|}{|q_2^2|} = \ln\frac{|q_2^2|_{\max}}{|q_2^2|_{\min}}.$$

In the integration over $|q_2^2|$ the lower limit is of kinematical origin, $|q_2^2|_{\min} = m_e^2y_2^2/(1-y_2)$, where

$$y_2 = \frac{2q_2p_1}{s} = \frac{\omega_2}{E_2} = \frac{W^2(1-x)+\mathbf{k}_\perp^2}{sx(1-x)}. \tag{22}$$

With the considered logarithmic accuracy the upper limit is determined by a scale at which the integrand (besides the photon propagator) starts to decrease significantly. For pion pair production this leads to

$$|q_2^2|_{\max} \sim \min\left\{\frac{\mathbf{k}_\perp^2}{1-y_2}, m_\rho^2, W^2\right\}, \tag{23}$$

where m_ρ is the ρ meson mass, which is the natural scale of the form factors. As a result, we have

$$\begin{aligned}\mathrm{d}\sigma_{12} &= -\frac{\alpha^3}{32\pi^4}\frac{\rho_2^{++}}{s^2W^2\mathbf{k}_\perp^2}L_2\mathrm{Re}(F_\pi^*T)\frac{\mathrm{d}^3p_+\mathrm{d}^3p_-}{\varepsilon_+\varepsilon_-},\\ T &= \sum_{ab} M_{ab}C_1^{ab}.\end{aligned} \tag{24}$$

The calculation of the trace (19) which determines C_1^{ab} is given in Appendix B.

To present the contribution (24) in a compact form, it is useful to introduce the auxiliary vector $\mathbf{r}_\perp$ and the angle ϕ between this vector and the vector $\mathbf{k}_\perp$ via[3]

$$\begin{aligned}\mathbf{r}_\perp &= \frac{1}{2}(\mathbf{\Delta}_\perp - \xi\mathbf{k}_\perp) = \frac{x_-}{x}\mathbf{p}_{+\perp} - \frac{x_+}{x}\mathbf{p}_{-\perp},\\ \mathbf{r}_\perp\mathbf{k}_\perp &= |\mathbf{r}_\perp||\mathbf{k}_\perp|\cos\phi\end{aligned} \tag{25}$$

[3] The angle ϕ is also the azimuthal angle between the vectors $\mathbf{p}_+$ and $(-\mathbf{p}_1)$ in the $\gamma^*\gamma$ c.m.s.

and use the dimensionless quantities

$$z_r = \frac{|\mathbf{r}_\perp|}{\mu}, \quad z_k = \frac{|\mathbf{k}_\perp|}{\mu}, \quad d = 1 - x + \frac{(1-\xi^2)z_k^2}{4(1+z_r^2)}. \tag{26}$$

In this notation

$$\begin{aligned}W^2 &= 4\mu^2\frac{1+z_r^2}{1-\xi^2}, \quad q_1^2 = -\mu^2\frac{z_k^2}{1-x},\\ y_2 &= \frac{4\mu^2}{s}\frac{(1+z_r^2)d}{x(1-x)(1-\xi^2)},\\ \frac{\mathrm{d}^3p_+\mathrm{d}^3p_+}{\varepsilon_+\varepsilon_-} &= 4\pi\mu^4 z_k\mathrm{d}z_k z_r\mathrm{d}z_r\mathrm{d}\phi\frac{\mathrm{d}x}{x}\frac{\mathrm{d}\xi}{1-\xi^2}.\end{aligned} \tag{27}$$

We obtain the following expression for the interference contribution $\mathrm{d}\sigma_{12}$:

$$\begin{aligned}\mathrm{d}\sigma_{12} &= \Big[G_{++}\mathrm{Re}\,(F_\pi^*M_{++}) + G_{+-}\mathrm{Re}\,(F_\pi^*M_{+-})\\ &\quad + G_{0+}\mathrm{Re}\,(F_\pi^*M_{0+})\Big]\frac{\mathrm{d}^3p_+\mathrm{d}^3p_-}{\varepsilon_+\varepsilon_-},\\ G_{ab} &= -\frac{\alpha^3}{8\pi^4}\frac{\rho_2^{++}L_2}{s^2W^2xz_kd}g^{ab},\\ g^{ab} &= \sum_{n=0}^{3} g_n^{ab}\cos(n\phi),\\ \rho_2^{++} &= \frac{2}{y_2^2}\left(1 - y_2 + \frac{1}{2}y_2^2\right),\\ L_2 &= \ln\frac{|q_2^2|_{\max}(1-y_2)}{m_e^2y_2^2}.\end{aligned} \tag{28}$$

The nonzero coefficients g_n^{ab} are

$$\begin{aligned}g_0^{++} &= (2-x)\xi z_k,\\ g_1^{++} &= (2-x)^2z_r - \frac{2-2x+x^2}{1-x}z_rd,\\ g_1^{+-} &= -(2-2x+x^2)z_r,\\ g_2^{+-} &= -(2-x)\xi z_k,\\ g_3^{+-} &= 2(d-1+x)z_r,\\ g_0^{0+} &= z_r(2-x)\sqrt{2(1-x)},\\ g_1^{0+} &= -2\xi z_k\sqrt{2(1-x)},\\ g_2^{0+} &= -\frac{2(2-x)}{\sqrt{2(1-x)}}(d-1+x)z_r.\end{aligned} \tag{29}$$

Let us briefly discuss this result.

We note that

$$\frac{\rho_2^{++}}{s^2} \propto \frac{1}{(sy_2)^2} = \frac{x(1-x)}{\left[W^2(1-x)+\mathbf{k}_\perp^2\right]^2}.$$

Therefore, the effect under discussion does not decrease with growing s, as one could imagine from a first look at (28).

The coefficient g^{0+} is of the same order as g^{++} and g^{+-}. Near the mass shell the amplitude $M_{0+} \propto \sqrt{-q_1^2} \sim$

$k_\perp$ [see (13) and (20)]. However, in the main region for the charge asymmetry the total transverse momentum of the pion system, $k_\perp$, is not small. Therefore the contribution of the amplitude M_{0+} to the interference is roughly of the same order of magnitude as the contributions of the other amplitudes.

The $\pi^+ \leftrightarrow \pi^-$ exchange is realized by the $\xi \to -\xi$ and $\phi \to \pi - \phi$ replacements. As was discussed above, the contribution $\mathrm{d}\sigma_{12}/(\mathrm{d}^3p_+\mathrm{d}^3p_-)$ is C-odd, i.e. it changes sign under this exchange. Indeed, the coefficients g^{++} and g^{+-} alter sign while g^{0+} remains unchanged. On the other hand, the amplitudes M_{++} and M_{+-} are unchanged (C-even) while M_{0+} changes sign (C-odd) [see (12)].

According to (28) and (29) the contribution of amplitude M_{+-} disappears after averaging over the azimuthal angle ϕ (this fact is explained in Appendix C):

$$\begin{aligned}\langle \mathrm{d}\sigma_{12}\rangle_\phi &\propto -g_0^{++}\mathrm{Re}\,(F_\pi^* M_{++}) - g_0^{0+}\mathrm{Re}\,(F_\pi^* M_{0+}) \\ &= -(2-x) \\ &\times \left[\xi z_k \; \mathrm{Re}\,(F_\pi^* M_{++}) + z_r\sqrt{2(1-x)}\mathrm{Re}\,(F_\pi^* M_{0+})\right].\end{aligned} \tag{30}$$

For small transverse momentum of the produced pair, $k_\perp \to 0$, our result for $\mathrm{d}\sigma_{12}$ coincides with that of [3] (see Appendix C). In this region the asymmetry in ξ is negligibly small compared with that in v.

We have obtained our equations in the dominant region of the effect $k_\perp^2 \sim -q_1^2 \lesssim W^2$. However, our sum $\sum g^{ab}\mathrm{Re}\,(F_\pi^* M_{ab})$ entering (28) coincides with the corresponding expression from [4] despite the fact that the latter was obtained in a quite different kinematical region (at $-q_1^2 \gg W^2$).

The term $\mathrm{d}\sigma_{13}$ is obtained from the presented formulae using the substitution rules (see Appendix C for details)

$$\begin{aligned}&\frac{\mathrm{d}\sigma_{13}}{\mathrm{d}^3p_+\mathrm{d}^3p_-} = \\ &-\frac{\mathrm{d}\sigma_{12}}{\mathrm{d}^3p_+\mathrm{d}^3p_-}(p_1 \leftrightarrow p_2, p_1' \leftrightarrow p_2', q_1 \leftrightarrow q_2);\end{aligned} \tag{31}$$

in particular

$$x_\pm \to y_\pm, \quad \xi \to \eta,$$
$$M_{ab}(q_1,q_2,\Delta) \to (-1)^{a+b}M_{ba}(q_1,q_2,\Delta).$$

5 Two-photon and bremsstrahlung background

Let us now present the necessary formulae for the two-photon ($\mathrm{d}\sigma_1$) and bremsstrahlung ($\mathrm{d}\sigma_2$) contributions to the pion pair production which are background for the considered asymmetry.

The differential cross section of the *two-photon contribution* can be written via the helicity amplitudes M_{ab} (10) as

$$\mathrm{d}\sigma_{C=+1} = \frac{(4\pi\alpha)^2}{q_1^2 q_2^2} \sum_{abcd=\pm1,0} M_{cd}^* M_{ab} \varrho_1^{ac} \varrho_2^{bd} \frac{\mathrm{d}\Gamma}{2s}. \tag{32}$$

Here ϱ_2^{bd} is defined in (18) and ϱ_1^{ac} is given by a similar expression with the evident changes $p_2 \to p_1$, $p_2' \to p_1'$, $e_2 \to e_1$.

The further calculations repeat those in Sect. 4. At fixed value of $\mathbf{k}_\perp$ there are two regions (A) and (B) where either $q_2^2 \approx 0$ or $q_1^2 \approx 0$. Those regions give the dominant contributions in logarithmic approximation:

$$\mathrm{d}\sigma_{C=+1} = \frac{\alpha^2}{32\pi^5 \mathbf{k}_\perp^2}(T_A + T_B)\frac{\mathrm{d}^3p_+\mathrm{d}^3p_-}{\varepsilon_+\varepsilon_-}. \tag{33}$$

In region (A) we can use (20)–(23), which leads to

$$T_A = \frac{\rho_2^{++}}{(sx)^2} L_2 \sum_{n=0}^{2} T_n \cos(n\phi). \tag{34}$$

The coefficients T_n are of the form

$$\begin{aligned}T_0 &= \frac{1}{2}\left(|M_{++}|^2 + |M_{+-}|^2\right)\left(1 - x + \frac{1}{2}x^2\right) \\ &\quad + |M_{0+}|^2(1-x), \\ T_1 &= -\mathrm{Re}\left[\left(M_{+-}^* - M_{++}^*\right)M_{0+}\right](2-x)\sqrt{\frac{1-x}{2}}, \\ T_2 &= -\mathrm{Re}\left(M_{+-}^* M_{++}\right)(1-x).\end{aligned} \tag{35}$$

The helicity amplitudes M_{ab} have be taken in the limit (20).

The contribution T_B of region (B) can be obtained from T_A substituting $p_1 \leftrightarrow p_2, p_1' \leftrightarrow p_2', q_1 \leftrightarrow q_2$ (similar to (31) but without changing sign).

A detailed analysis of these equations [8] shows that the pairs produced via the two-photon mechanism are concentrated at small values of $k_\perp$:

$$\mathrm{d}\sigma_{C=+1} \propto \frac{\mathrm{d}\mathbf{k}_\perp^2}{\mathbf{k}_\perp^2} \ln\frac{\mathbf{k}_\perp^2 s}{m_e^2 W^2}, \tag{36}$$

and they are distributed almost uniformly in the rapidity:

$$\mathrm{d}\sigma_{C=+1} \propto \frac{\mathrm{d}x}{x}\frac{\mathrm{d}y}{y}. \tag{37}$$

For the *bremsstrahlung contribution* ($\mathrm{d}\sigma_{C=-1} = \mathrm{d}\sigma_2 + \mathrm{d}\sigma_3$) we use the results of [9]. For pions flying along electrons, the dominant contribution is given by the amplitude $\mathcal{M}_2$ taken in the limit (20). In logarithmic approximation we have

$$\begin{aligned}\mathrm{d}\sigma_2 &= |\mathcal{M}_2|^2\frac{\mathrm{d}\Gamma}{2s} = \frac{\alpha^4}{8\pi^3}|F_\pi|^2 \\ &\times \frac{x^2\rho_2^{++}}{W^2[W^2(1-x) + \mathbf{k}_\perp^2 + m_e^2 x^2]^2} LT_- \frac{\mathrm{d}^3p_+\mathrm{d}^3p_-}{\varepsilon_+\varepsilon_-}, \\ T_- &= \left(1 - \frac{4\mu^2}{W^2}\right)\left[y^2 + \left(y_2 - \frac{W^2}{s}\right)^2\right] \\ &\quad - y^2\eta^2 - (y\eta + y_2 x\xi)^2, \\ L &= \ln\frac{s^2(1-x)(1-y_2)}{m_e^2[W^2 + s y_2(1-x)]}.\end{aligned} \tag{38}$$

The denominator $[W^2(1-x) + \mathbf{k}_\perp^2 + m_e^2 x^2]^2$ shows that this contribution is dominated by small $\mathbf{k}_\perp^2$ and large x (i.e. $1 - x \ll 1$).

For pions flying along positrons the corresponding contribution $\mathrm{d}\sigma_3$ is obtained via $\mathrm{d}\sigma_3 = \mathrm{d}\sigma_2(x \leftrightarrow y, y_2 \leftrightarrow x_1, \xi \leftrightarrow \eta)$.

6 The $\gamma^*\gamma \to \pi^+\pi^-$ subprocess

For the pion pair production the strong interaction effects are of primary interest. Nevertheless, the pure *Born QED model* (point-like pions) gives a reasonable description of the squared two-photon amplitude at $W \lesssim 1\,\mathrm{GeV}$. On the contrary, the QED amplitude itself is real whereas the phase shifts of the correct $\gamma\gamma \to \pi^+\pi^-$ amplitudes coincide with those of elastic $\pi\pi$ scattering (at least, at $W < 520$ MeV). The QED amplitudes M_{ab} entering (24) are (see Appendix A)

$$\begin{aligned} M_{++}^{\mathrm{QED}} &= 8\pi\alpha - M_{+-}^{\mathrm{QED}}, \\ M_{+-}^{\mathrm{QED}} &= 8\pi\alpha \frac{(1-x)z_r^2}{(1+z_r^2)d}, \\ M_{0+}^{\mathrm{QED}} &= 4\pi\alpha\xi \frac{\sqrt{-2q_1^2}}{\mu} \frac{(1-x)(d-2+2x)z_r}{(1+z_r^2)d^2}, \\ F_\pi^{\mathrm{QED}} &= 1. \end{aligned} \tag{39}$$

In the next section we obtain numerical results for that model. It allows us to develop a better understanding of the potentiality of future experiments.

With increasing dipion effective mass W above the threshold the strong interaction effects become more essential. At $W \gtrsim 1\,\mathrm{GeV}$ these effects dominate and the main contribution is given by resonances. The pion form factor entering the bremsstrahlung amplitude is experimentally well studied using the reaction $e^+e^- \to \pi\pi$. Using the charge asymmetry the main task in this domain is to study the resonances in the two-photon channel, i.e. the different f_0's and f_2. The nature of the f_0 resonances has been subject of discussion till now, and different models of the resonance origin can lead to different W-dependences of their phases. Those models can be tested using the discussed asymmetry. For the f_2 resonance the value of its amplitude for the two-photon production with total helicity 0 can be obtained by studying the longitudinal charge asymmetry (which practically does not depend on the amplitude with total initial helicity 0).

Near the resonances some of the amplitudes M_{ab} are enhanced compared to their QED values. Besides, we have for the pion form factor $|F_\pi(W^2)| > 1$ in a wide enough region of interest. A detailed study of the effect with a realistic $\gamma\gamma \to \pi^+\pi^-$ amplitude and a discussion of the potentiality of such experiments to study the phase shifts of $\pi\pi$ scattering and the resonance nature will be presented elsewhere.

7 Analysis of results

7.1 Studied quantities

As was discussed before, the contribution $\mathrm{d}\sigma_{12}$ dominates for pion pairs flying along the initial electron, i.e. at large values of x. On the other hand, $\mathrm{d}\sigma_{13}$ dominates for dipions flying along the initial positron, i.e. at large values of y. Since $xy = (W^2 + \mathbf{k}_\perp^2)/s$, we can introduce the characteristic value

$$x_0 = \sqrt{\frac{W^2 + \mathbf{k}_\perp^2}{s}} \tag{40}$$

and find that the total longitudinal momentum of the pion pair in the c.m.s. of the colliding electrons and positrons $k(p_2 - p_1)/s^{1/2} \propto x - y$ is positive at $x > x_0$ and negative at $x < x_0$. Therefore, $|\mathrm{d}\sigma_{12}| \gg |\mathrm{d}\sigma_{13}|$ at $x \gg x_0$ and $|\mathrm{d}\sigma_{13}| \gg |\mathrm{d}\sigma_{12}|$ at $x \ll x_0$.

In the region $x \sim y \sim x_0$ the two contributions are of the same order, $|\mathrm{d}\sigma_{12}| \sim |\mathrm{d}\sigma_{13}|$, but their distributions over the longitudinal variable K_- and the transverse variable v have different properties. Indeed, K_- is antisymmetric whereas v is symmetric under $p_1 \leftrightarrow p_2$ exchange. Having in mind relation (31), we conclude that

$$\frac{\mathrm{d}\sigma_{13}}{\mathrm{d}K_-} = \frac{\mathrm{d}\sigma_{12}}{\mathrm{d}K_-}(p_1 \leftrightarrow p_2, p_1' \leftrightarrow p_2', q_1 \leftrightarrow q_2),$$

$$\frac{\mathrm{d}\sigma_{13}}{\mathrm{d}v} = -\frac{\mathrm{d}\sigma_{12}}{\mathrm{d}v}(p_1 \leftrightarrow p_2, p_1' \leftrightarrow p_2', q_1 \leftrightarrow q_2).$$

To take into account the described properties and to summarize different contributions, it is natural to introduce the following quantities related to the charge asymmetry of the pions[4]:

$$\Delta\sigma_K = \int\limits_{\mathcal{D}} \epsilon(K_-)\mathrm{d}\sigma, \quad \Delta\sigma_v = \int\limits_{\mathcal{D}} \epsilon(v)\epsilon(x-y)\mathrm{d}\sigma. \tag{41}$$

In these definitions we denote by $\mathcal{D}$ the kinematical region in phase space given by the detector array and suitably chosen cuts (certainly, it is necessary to test that this region is symmetric in K_- and v).

The background for these effects is found integrating the two-photon and bremsstrahlung contributions over the same region $\mathcal{D}$:

$$\Delta\sigma_B = \int\limits_{\mathcal{D}} \left(\mathrm{d}\sigma_{C=+1} + \mathrm{d}\sigma_{C=-1}\right). \tag{42}$$

7.2 Numerical analysis

Below we consider the charge asymmetry effects within the QED model of point-like pions. First, we present in Table 1

[4] Below we use the standard step functions $\theta(x)$ and $\epsilon(x) = \theta(x) - \theta(-x)$. For example, $\Delta\sigma_K$ is the difference between cross sections for events with $p_{+z} > p_{-z}$ and that with $p_{+z} < p_{-z}$ in the e^+e^- c.m.s.

Table 1. Pion charge asymmetry signals and background at different c.m. energies

$\sqrt{s}$, GeV	1	4	10	200
$\Delta\sigma_K$, pb	−6.1	−26	−35	−56
$\Delta\sigma_v$, pb	3.3	17	27	51
$\Delta\sigma_B$, pb	420	2900	6200	27000

the integrated pion charge asymmetry in the variables K_- and v (signals S) and the background of two-photon and bremsstrahlung production (background B) at different c.m. energies $s^{1/2}$.

Using the charge asymmetry one can study the two-photon amplitude and its phase shift as a function of the effective mass of the $\pi^+\pi^-$ system $W = \sqrt{k^2}$. To see the potentiality of such a study, we present in Fig. 4 the distribution of the signal and the background over W for two collider energies. Both signal and background are concentrated near the threshold where the longitudinal asymmetry $|\mathrm{d}\Delta\sigma_K/\mathrm{d}W|$ is considerably larger than the transverse one, $|\mathrm{d}\Delta\sigma_v/\mathrm{d}W|$. At $W > 400 \div 500\,\mathrm{MeV}$ (depending on $s^{1/2}$) the transverse asymmetry dominates over the longitudinal one. Nevertheless, having in mind the results for the muon charge asymmetries presented below we mainly discuss in the following the longitudinal asymmetry.

We consider two typical intervals of effective mass values (over which we integrate):

(1) $W = 300 \div 350\,\mathrm{MeV}$; this is near the threshold where QED is approximately valid.
(2) $W = 475 \div 525\,\mathrm{MeV}$. This is far from the threshold and resonances where one hopes to describe the modules of the two-photon amplitudes reasonably within QED whereas the bremsstrahlung amplitude is enhanced compared to its QED value due to the ρ meson resonance. For this region we expect that our numbers underestimate the effect.

The signal/background ratio (S/B) is introduced by

$$\frac{S}{B} = \frac{|\Delta\sigma_S|}{\Delta\sigma_B} \quad \text{with} \quad S = K_-, v. \tag{43}$$

Besides, it is useful to consider the statistical significance (SS) of the effect. This quantity is expressed via the number of events for the effect, $N_S = \mathcal{L}|\Delta\sigma_S|$, and background, $N_B = \mathcal{L}\Delta\sigma_B$, as

$$SS = \frac{N_S}{\sqrt{N_B}}, \tag{44}$$

where $\mathcal{L}$ is the integrated luminosity of the collider. For the luminosity we use numbers proposed for the DAΦNE and PEP II colliders. We now demonstrate that the S/B and SS quantities can be considerably improved with suitable cuts on $k_\perp$ and x.

The variable $\mathbf{k}_\perp^2$ describes both the transverse motion of the dipion and the virtuality of the photon. The charge asymmetry effect, see (28) and (29), vanishes at small $|\mathbf{k}_\perp|$, $\mathrm{d}\sigma_{12} \propto \mathrm{d}|\mathbf{k}_\perp|$. On the contrary, the two-photon contribution is singular at $|\mathbf{k}_\perp| \sim 0$, see (36). In Fig. 5 we present the signal and background integrated over $k_\perp > k_0$ (k_0 being a cut-off from below). One observes that with increasing k_0 the background drops considerably faster than the signal. Therefore, some cut at small $\mathbf{k}_\perp^2 = k_0^2$ is desirable; the best cut on the pair transverse momentum k_0 depends on s and W^2.

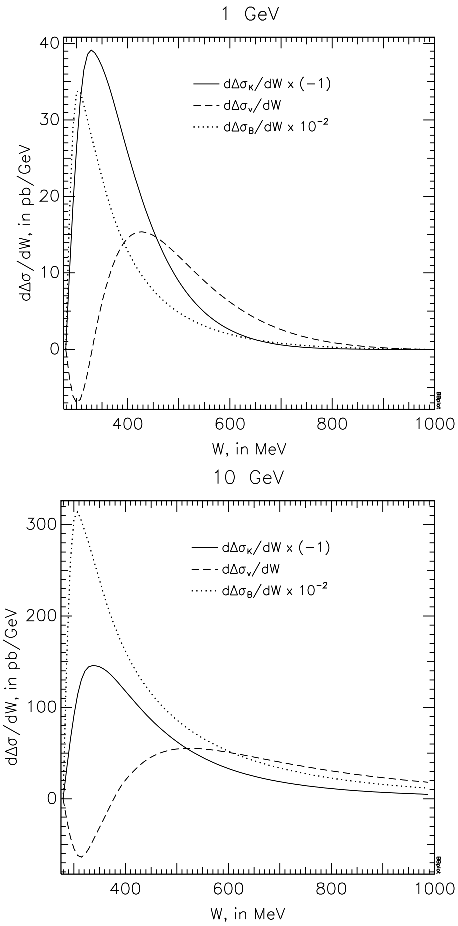

Fig. 4. Contributions $\Delta\sigma_K$ and $\Delta\sigma_v$ (41) and background at $s^{1/2} = 1$ and 10 GeV versus W

The variable x describes the dipion motion along the collision axis. The factor $W^2 d \equiv W^2(1-x) + \mathbf{k}_\perp^2$ in the denominator of (28) shows that in the interference the dipions tend to be concentrated at $x \sim 1$. On the contrary, in the two-photon production the x-distribution of the dipions is proportional to $1/x$. Therefore, some cut at not too low x would be desirable. On the other hand, the bremsstrahlung contribution is concentrated near $x = 1$ more strongly than the charge asymmetry contribution. Moreover, the values of x very close to 1 contribute only weakly to the charge asymmetry. Therefore, an additional cut at x near 1 is suggested. In Fig. 6 these features are demonstrated for signal and background contributions integrated over $x > x_0$.

To show the effect of both cuts we present in Table 2 some examples considering cuts in $k_\perp$ and two symmetri-

Table 2. Effect of cuts in $k_\perp$ and x, y

$\sqrt{s}$	$\mathcal{L}$ fb^{-1}	W MeV	cuts	$\Delta\sigma_B$ pb	$\Delta\sigma_K$ pb	S/B %	SS
1 GeV	5	300	no cuts	145	−1.85	1.3	11
DAΦNE		$\div$	$k_\perp > 100\,\mathrm{MeV}$,	14.6	−1.07	7.3	20
		350	$0.4 < x, y < 0.9$				
10 GeV	30	475	no cuts	433	−3.13	0.72	8.2
PEP-II		$\div$	$k_\perp > 150\,\mathrm{MeV}$,	17.2	−1.62	9.5	68
		525	$0.3 < x, y < 0.95$				

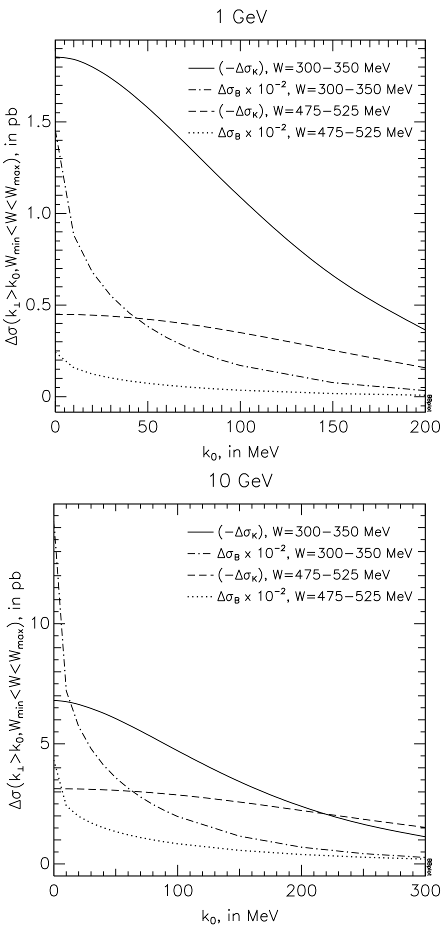

Fig. 5. Contributions $\Delta\sigma_K$ and background at $s^{1/2} = 1$ and 10 GeV for the interval $W = 300 \div 350\,\mathrm{MeV}$ and $W = 475 \div 525\,\mathrm{MeV}$ and $k_\perp > k_0$ versus k_0

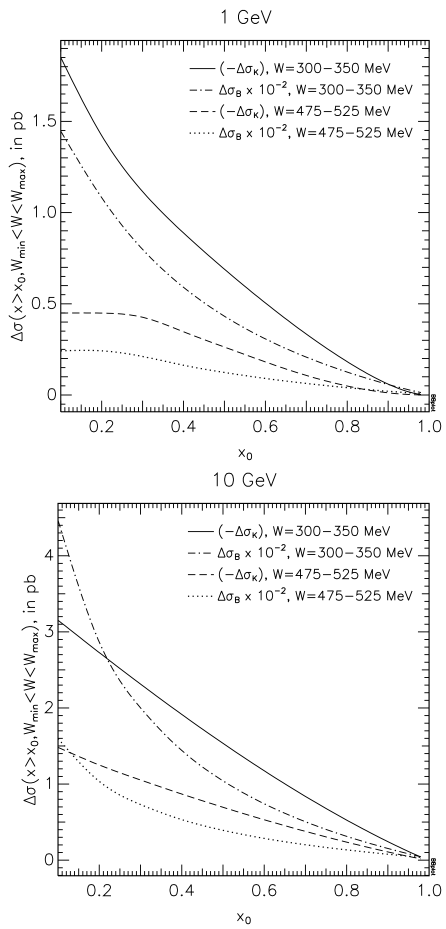

Fig. 6. The contributions $\Delta\sigma_K$ and background at $s^{1/2} = 1$ and 10 GeV for the intervals $W = 300 \div 350\,\mathrm{MeV}$ and $W = 475 \div 525\,\mathrm{MeV}$ and $x > x_0$ versus x_0

cal regions in pion rapidity (contributions of pions flying along the initial electron momentum $x_1 > x > x_2$ and the initial positron momentum $x_1 > y > x_2$). For the DAΦNE collider we consider the region of small effective mass of the dipion $W = 300 \div 350\,\mathrm{MeV}$. The used cuts improve S/B by a factor about 5 and SS by a factor of about 2. For the PEP-II collider we consider an intermediate mass region $W = 475 \div 525\,\mathrm{MeV}$. The used cuts improve both S/B and S/S by about one order of magnitude. It is natural to expect that the same type of improvement will take place at $W \sim 1\,\mathrm{GeV}$.

For the physical analysis of the results it is useful to consider the individual contributions of different helicity amplitudes M_{ab} to the charge asymmetry. The results for the longitudinal asymmetry $\mathrm{d}\Delta\sigma_K/\mathrm{d}W$ are shown in Fig. 7. In this distribution the amplitude M_{++} is dominant whereas M_{+-} contributes only weakly to the asymmetry (in accordance with the discussion at the end of Sect. 4). The last contribution can be even stronger suppressed, ex-

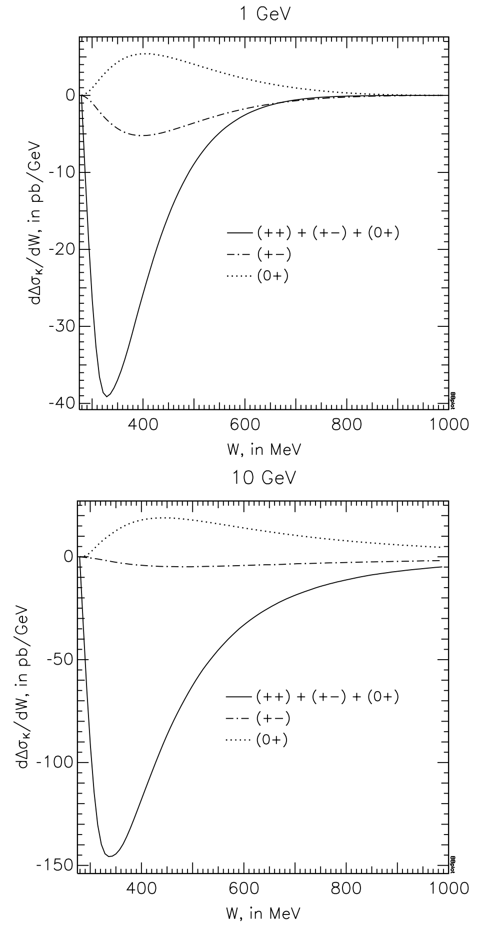

Fig. 7. Contributions of the helicity amplitudes $M_{ab} \equiv (ab)$ to the distribution $\mathrm{d}\Delta\sigma_K/\mathrm{d}W$ (41) versus W at $s^{1/2} = 1$ and 10 GeV

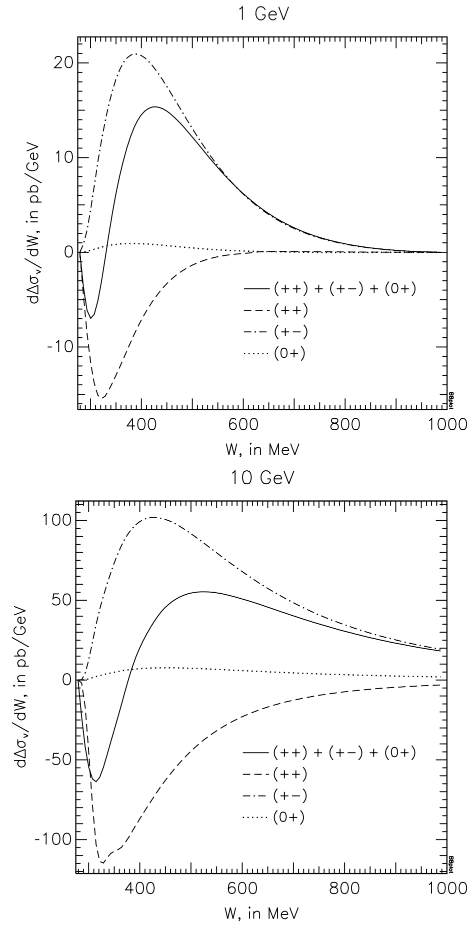

Fig. 8. Same as in Fig. 7 for the distribution $\mathrm{d}\Delta\sigma_v/\mathrm{d}W$, see (41)

cluding pion pairs with small longitudinal momentum in the e^+e^- c.m.s. additionally. Therefore, the distribution over K_- allows us to obtain clean information about the amplitude M_{++}.

In the transverse distribution $\mathrm{d}\Delta\sigma_v/\mathrm{d}W$ (Fig. 8) the contribution of the M_{++} and M_{+-} amplitudes are of the same order, partially compensating each other. Therefore, the combined distributions over K_- and v can give complementary knowledge about individual contributions of the M_{++} and M_{+-} helicity amplitudes.

Finally let us notice, that in the K_--distribution the contribution of the amplitude with one scalar photon M_{0+} is not negligible.

7.3 Weighted cross sections

For future studies it is useful to look at the presented analysis from a more general point of view. The distributions of produced pions contain a charge asymmetric part. To extract it, we consider each event with the C-odd weight function $\epsilon(K_-)$ or $\epsilon(v)$. So, our asymmetry $\Delta\sigma_K$ and $\Delta\sigma_v$ defined in (41) can be considered as "weighted cross sections" with these weights. Certainly, to extract the asymmetric part of the cross section, one can use also other C-odd weight functions. It seems to be attractive to explore more smooth weight functions, for example, given by factors K_- and v instead of $\epsilon(K_-)$ and $\epsilon(v)$, i.e. to introduce weighted cross sections

$$\Delta\sigma_K^C = \int\limits_{\mathcal{D}} K_- \mathrm{d}\sigma, \quad \Delta\sigma_v^C = \int\limits_{\mathcal{D}} v\varepsilon(x-y)\mathrm{d}\sigma. \tag{45}$$

They (or similar quantities) may be more suitable for a theoretical analysis, for generalizations and for data processing. In particular, the signs of small differences $p_{+z} - p_{-z}$ or $\mathbf{p}_{+\perp}^2 - \mathbf{p}_{-\perp}^2$ cannot be reliably established from the data. However, the proposed weighted cross sections (45) are weakly sensitive to those small values.

The background for these "cross sections" is given by the total weighted cross section of the process in the same kinematical region,

$$\begin{aligned} \Delta\sigma_{BK}^C &= \int\limits_{\mathcal{D}} |K_-| \left(\mathrm{d}\sigma_{C=+1} + \mathrm{d}\sigma_{C=-1}\right), \\ \Delta\sigma_{Bv}^C &= \int\limits_{\mathcal{D}} |v| \left(\mathrm{d}\sigma_{C=+1} + \mathrm{d}\sigma_{C=-1}\right). \end{aligned} \tag{46}$$

Table 3. Muon pair charge asymmetry signals and background at different c.m. energies

$\sqrt{s}$, GeV	1	4	10	200
$\Delta\sigma_K$, pb	-11	7.9	42	120
$\Delta\sigma_v$, pb	180	660	950	1700
$\Delta\sigma_B$, pb	7100	3.7×10^4	6.9×10^4	3.7×10^5

8 Process $e^-e^+ \to e^-e^+\mu^+\mu^-$

The process $e^-e^+ \to e^-e^+\mu^+\mu^-$ can give an essential background while studying the dipion production.

The charge asymmetry of muons in this process has been studied for the first time at small $k_\perp$ in [3]. The muon asymmetry without that limitation was obtained in [10] (in the same logarithmic accuracy as is used here). We use the results as given in the review of [11] and transform them to a form convenient for analysis[5]. In the notations of (25) and (26) (where μ is now the muon mass) we have

$$\begin{aligned}
\mathrm{d}\sigma_{12} &= \frac{2\alpha^4}{\pi^3}\frac{\rho_2^{++}L_2}{s^2W^2xz_k(1+z_r^2)d^2} \\
&\quad\times\left[\sum_{n=0}^{3} t_n\cos(n\phi)\right]\frac{\mathrm{d}^3p_+\mathrm{d}^3p_-}{\varepsilon_+\varepsilon_-}, \qquad (47)\\
t_0 &= t_2 + (2-x)\xi z_k d,\\
t_1 &= \frac{z_r}{4}\left\{(1-x)\left[8(1-x)+10(1-\xi^2)z_k^2\right]\right.\\
&\quad + (2-2x+x^2)\left[\frac{d-1+x}{1-x}(1+\xi^2)z_k^2\right.\\
&\quad \left.\left.+\ 4\left(-(d-2+2x)+(1-x)\frac{1+\xi^2}{1-\xi^2}(1+z_r^2)\right)\right]\right\}\\
t_2 &= (2-x)\xi(d-2+2x)z_kz_r^2,\\
t_3 &= 2(1-x)(d-1+x)z_r^3,
\end{aligned}$$

with L_2 given by (28) and $|q_2^2|_{\max} \sim \min\{\mathbf{k}_\perp^2/(1-y_2), W^2\}$. At small transverse momentum of the pair $k_\perp$ this result coincides with that obtained in [3] (see Appendix C). The contribution $\mathrm{d}\sigma_{13}$ is obtained from $\mathrm{d}\sigma_{12}$ using the replacements (31).

The two-photon and bremsstrahlung backgrounds can be found in review [11].

We have analyzed the charge asymmetry of muons in the same terms as it was done for the pions. Table 3 contains values of integrated signals and background at different c.m. energies. From that table we observe:

(i) the muon transverse asymmetry $\Delta\sigma_v$ is considerably larger than the muon longitudinal asymmetry $\Delta\sigma_K$;
(ii) the transverse asymmetry for muons is considerably larger than that for pions (see Table 1);
(iii) the longitudinal asymmetries for pions and muons are of the same order of magnitude.

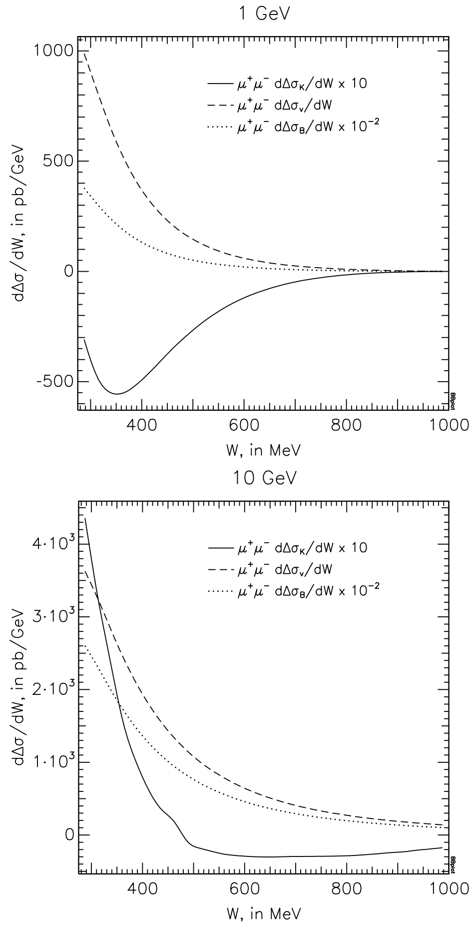

Fig. 9. Contributions $\Delta\sigma_K$ and $\Delta\sigma_v$ (41) and background at $s^{1/2} = 1$ and 10 GeV versus W for muon pair production

Similar relations between muon and pion asymmetries take place in all considered regions of the parameters. Moreover, in some regions the longitudinal asymmetry of muons disappears contrary to that of pions. In Figs. 9 and 10 we present the distributions similar to those given in Figs. 4 and 5 for pions. Having in mind the muon production as a possible background for the pion production, we consider just the same regions of W as used for pions. It is interesting to note that at $s^{1/2} = 10$ GeV the longitudinal asymmetry $\mathrm{d}\Delta\sigma_K/\mathrm{d}W$ (Fig. 9) changes sign at $W \approx 500$ MeV. The position of this crossover depends on $s^{1/2}$ (cf. the curve for $s^{1/2} = 1$ GeV). Such a sign change is absent for pions.

9 Summary and conclusions

We have calculated the charge asymmetry contribution $\mathrm{d}\sigma_{\mathrm{interf}}/(\mathrm{d}^3p_+\mathrm{d}^3p_-)$ for the process $e^+e^- \to e^+e^-\pi^+\pi^-$. Our result, summarized in (28), (29) and (31), is expressed via the helicity amplitudes M_{++}, M_{+-} and M_{0+} of the subprocess $\gamma^*\gamma \to \pi^+\pi^-$ and the pion form factor F_π in

[5] Note two misprints in [11]: First, diagram (b) in Fig. 4.1 should be replaced by diagram (c) and vice versa. Second, in the statement after (4.36) "dσ_{ac} may be derived from (4.36) through the substitution (4.4)" one has to add "changing the overall sign" - see Appendix C for the pion case

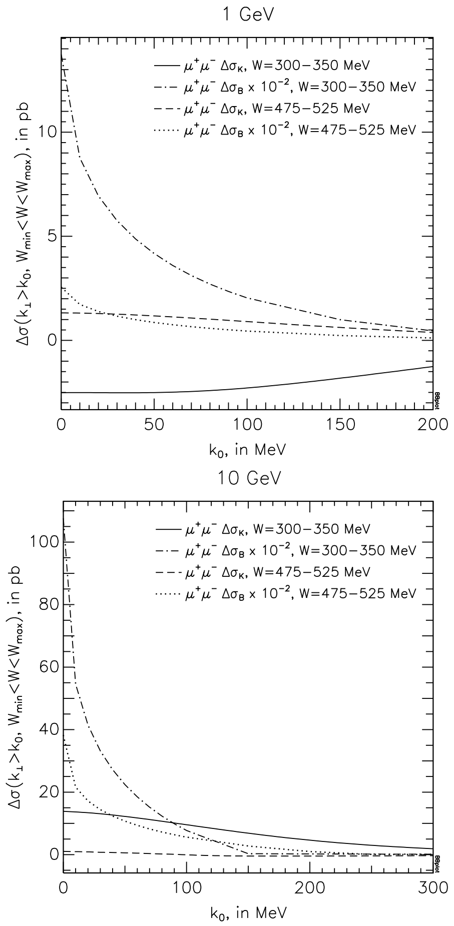

Fig. 10. The contribution $\varDelta\sigma_K$ and background at $s^{1/2} = 1$ and 10 GeV for the intervals $W = 300 \div 350$ MeV and $W = 475 \div 525$ MeV and $k_\perp > k_0$ versus k_0 for muon pair production

analytical form. It can be used for experiments both without recording the scattered electrons (no tag experiments) and with recording one scattered electron (single tag experiments).

The experimentally observable effects can be studied, in principle, in the longitudinal asymmetry (in the variable K_- of (8) representing the difference in longitudinal momenta of positive and negative pions) and in the transverse asymmetry (in the variable v of (8) representing the difference between squared transverse momenta of positive and negative pions). The longitudinal asymmetry effects are saturated mainly by the contribution of the $\gamma\gamma \to \pi^+\pi^-$ helicity amplitude M_{++}. The main contribution to the transverse asymmetry is given by amplitudes M_{++} and M_{+-}. The two-photon amplitude M_{0+} (one longitudinal (scalar) photon and one transverse photon) gives typically about 10% of effect (within the QED model).

The main part of our numerical analysis of the effect is performed in the QED model giving a reasonable description of the two-photon amplitude at $W \lesssim 1$ GeV and the one-photon amplitude near the threshold.

We have considered also the charge asymmetry for muon pairs which can give an essential background to the pion asymmetry effects. Our analysis demonstrates that the transverse asymmetry of pions is much smaller than that of muons, whereas the longitudinal asymmetry of pions is generally close to that of muons (in some regions of parameters the latter even disappears). Therefore, in our detailed numerical studies we have concentrated our efforts to the study of the longitudinal asymmetry.

Our QED numerical analysis presents a good basis to estimate the potentiality for studying pion–pion scattering phase shifts near the threshold at the colliders DA$\varPhi$NE, VEPP2000, etc. The study of resonances (for example, different f_0's and f_2) at the colliders PEP-II and KEK-B requires more detailed estimates which are in progress.

The values of the signal to background ratio S/B (43) obtained in the QED model are typically around 1%. However, with the expected high luminosity of B- and ϕ-factories the statistical significance of the effect SS (44) is high enough (typically about 10) for the considered ideal case when all dipions are assumed to be recorded. The strongly different dependence of signal and background on the components of the total dipion momentum results in a large improvement of both S/B and SS (by about a factor 10 for $W \sim 0.5 \div 1$ GeV at the PEP-II) at suitable cuts in the total transverse momentum of pion pair $k_\perp$ and its total rapidity (see Table 2). With these estimates the perspectives of experiments look well.

The charge asymmetry in the resonance region will be considered elsewhere. Preliminary estimates indicate that the effect will be observable. Moreover, the quick change of the phase near the resonance results in a strong dependence of the asymmetry on W in this region; this could help to distinguish resonance models.

Finally, note that the presented equations for the muon charge asymmetry (47) can be used to estimate the production of c quarks in the process $e^+e^- \to e^+e^-c\bar{c}$ with production of open charm. The deviation from the QED result will be caused by violation of quark–hadron duality due to strong interactions. These deviations are expected to be large near the threshold where the $c\bar{c}$ resonance production is essential in both p- and s-waves. Simple QED calculations with an additional charge factor 8/9 give $\varDelta\sigma_v \sim 0.27$ pb at $s^{1/2} = 10$ GeV and about 4.1 pb at $s^{1/2} = 200$ GeV (here we put the c quark mass to 1.75 GeV to take into account the threshold for the production of open charm).

Acknowledgements. We are very grateful to A. Bondar, V. Fadin, I. Ivanov, E. Kuraev, V. Savinov, V. Serebryakov, W. Speth and V. Zhilich for useful discussions. This work was partially supported by grants RFBR 00-02-17592, 00-15-96691, "Universities of Russia" 015.0201.16, and Sankt-Petersburg Center of Higher education. V.G.S. acknowledges a support of Sächsisches Staatsministerium für Kunst und Wissenschaft, grant 4-7531.50-04-0361-00/25 and kind hospitality of NTZ of Leipzig university.

Appendix A
Kinematics of the process $\gamma^*\gamma^* \to \pi^+\pi^-$

Due to 4-momentum conservation $q_1 + q_2 = p_+ + p_-$, the amplitude $M^{\mu\nu}$ of the process $\gamma^*\gamma^* \to \pi^+\pi^-$ depends only on three independent momenta $q_1, q_2, \Delta = p_+ - p_-$. We use the Mandelstam variables

$$W^2 = (q_1+q_2)^2, \quad t = (q_1-p_+)^2, \quad u = (q_1-p_+)^2,$$

with the relations

$$W^2 + t + u = 2\mu^2 + q_1^2 + q_2^2, \quad t - u = -2q_1\Delta = 2q_2\Delta.$$

The polarization properties of the virtual photons are described by two polarization 4-vectors, $e_1^{(a)}$ and $e_2^{(b)}$, with helicities $a, b = \pm 1, 0$. For scalar (longitudinal) photons ($a = b = 0$) we use the following polarization vectors:

$$\begin{aligned} e_{1\mu}^{(0)} &= \sqrt{\frac{-q_1^2}{X}}\left(q_{2\mu} - \frac{q_1q_2}{q_1^2}q_{1\mu}\right), \\ e_{2\nu}^{(0)} &= \sqrt{\frac{-q_2^2}{X}}\left(q_{1\nu} - \frac{q_1q_2}{q_2^2}q_{2\nu}\right), \\ X &= (q_1q_2)^2 - q_1^2q_2^2. \end{aligned} \tag{A.1}$$

The transverse photons ($a, b = \pm 1$) can be described by two independent polarization vectors only. This choice can be realized by taking those vectors in the $\gamma^*\gamma^*$ center-of-mass system in the form

$$e_1^{(\pm)} = e_2^{(\mp)} = \mp\frac{1}{\sqrt{2}}(0, 1, \pm\mathrm{i}, 0). \tag{A.2}$$

To construct the corresponding covariant expression, we introduce a metric tensor of the subspace which is orthogonal to the 4-vectors q_1 and q_2

$$\begin{aligned} R_{\mu\nu} = g_{\mu\nu} - \frac{1}{X}\Big[&(q_1q_2)\,(q_{1\mu}q_{2\nu} + q_{1\nu}q_{2\mu}) \\ &- q_1^2q_{2\mu}q_{2\nu} - q_2^2q_{1\mu}q_{1\nu}\Big] \end{aligned}$$

and define two 4-vectors in that subspace (both of them antisymmetric under $p_+ \leftrightarrow p_-$ exchange)

$$\begin{aligned} r^\mu = \frac{1}{2}R^{\mu\nu}\Delta_\nu, \quad s^\mu &= \varepsilon^{\mu\nu\alpha\beta}\Delta_\nu q_{1\alpha}q_{2\beta}, \\ r^\mu s_\mu &= 0. \end{aligned} \tag{A.3}$$

In the $\gamma^*\gamma^*$ c.m.s. the tensor $R_{\mu\nu}$ has only two nonzero components $R_{xx} = R_{yy} = -1$. Both 4-vectors r^μ and s^μ have only nonzero components in the x and y directions and are perpendicular to each other[6]. Therefore, we can choose the x- and y-axes along these 4-vectors:

$$e_\mu^{(x)} = \frac{r_\mu}{\sqrt{-r^2}}, \qquad e_\mu^{(y)} = \frac{s_\mu}{\sqrt{-s^2}}. \tag{A.4}$$

[6] In the $\gamma^*\gamma^*$ c.m.s. the nonzero components of the 4-vector r coincides with the transverse components of the vector $\mathbf{p}_{+\perp}$ or with the transverse components of the vector $(-\mathbf{p}_{-\perp})$

In the $\gamma^*\gamma^*$ c.m.s. $e^{(x)} = (0,1,0,0)$, $e^{(y)} = (0,0,1,0)$. As a result, the covariant expression for the vectors (A.2) takes the form

$$e_{1\mu}^{(\pm)} = e_{2\mu}^{(\mp)} = \mp\frac{1}{\sqrt{2}}\left(e_\mu^{(x)} \pm \mathrm{i}e_\mu^{(y)}\right). \tag{A.5}$$

We define the helicity amplitudes for the discussed process as

$$M_{ab} = e_{1\mu}^{(a)}e_{2\nu}^{(b)}M^{\mu\nu},$$

where the inverse transformation is given in (10). Taking into account parity conservation, we obtain

$$\begin{aligned} M_{++} &= M_{-}, \qquad M_{+-} = M_{-+}, \\ M_{0+} &= -M_{0-}, \qquad M_{+0} = -M_{-0}. \end{aligned} \tag{A.6}$$

Since under $\pi^+ \leftrightarrow \pi^-$ exchange the C-even amplitude $M^{\mu\nu}$ is symmetric whereas the 4-vectors $e_{1,2}^{(\pm)}$ are antisymmetric [cf. (11)], the amplitudes M_{++}, M_{+-} and M_{00} are symmetric and the amplitudes M_{0+} and M_{+0} are antisymmetric under that exchange [see (12)].

Under photon exchange ($q_1 \leftrightarrow q_2$) the polarization vectors have to replaced by $e_1^{(0)} \to e_2^{(0)}$, $e^{(x)} \to e^{(x)}$, $e^{(y)} \to -e^{(y)}$, $e_1^{(\pm)} \to -e_2^{(\pm)}$, which can in a short-hand way be written as

$$e_1^{(a)} \to (-1)^a e_2^{(a)}.$$

Taking into account $M^{\mu\nu}(q_1, q_2, \Delta) = M^{\nu\mu}(q_2, q_1, \Delta)$, we obtain

$$M_{ab}(q_1, q_2, \Delta) \to (-1)^{a+b}M_{ba}(q_1, q_2, \Delta). \tag{A.7}$$

It is useful to present these amplitudes for the pure QED case (point-like pions):

$$\begin{aligned} M_{++}^{\mathrm{QED}} &= 8\pi\alpha - M_{+-}^{\mathrm{QED}}, \\ M_{+-}^{\mathrm{QED}} &= -8\pi\alpha\frac{r^2(W^2 - q_1^2 - q_2^2)}{(t-\mu^2)(u-\mu^2)}, \\ M_{+0}^{\mathrm{QED}} &= -2\pi\alpha\sqrt{\frac{2q_2^2r^2}{X}}\frac{(t-u)(W^2 + q_2^2 - q_1^2)}{(t-\mu^2)(u-\mu^2)}, \\ M_{0+}^{\mathrm{QED}} &= -2\pi\alpha\sqrt{\frac{2q_1^2r^2}{X}}\frac{(t-u)(W^2 + q_1^2 - q_2^2)}{(t-\mu^2)(u-\mu^2)}, \end{aligned} \tag{A.8}$$

with

$$r^2 = -\frac{W^2}{4X}\left[(t-\mu^2)(u-\mu^2) - q_1^2q_2^2\right] + \mu^2 < 0. \tag{A.9}$$

In the $\gamma^*\gamma^*$ cms the quantity $(-r^2)$ is the squared transverse momentum of π^+ or π^-.

Appendix B
Calculation of traces

B.1 Sudakov variables

When calculating the trace (19), we neglect the electron mass m_e and decompose any 4-vector A into components in the plane of the 4-vectors p_1 and p_2 and in the plane orthogonal to them:

$$A = x_A p_1 + y_A p_2 + A_\perp, \qquad (B.1)$$
$$x_A = \frac{2p_2 A}{s}, \quad y_A = \frac{2p_1 A}{s}, \quad A^2 = s x_A y_A + A_\perp^2.$$

The parameters x_A and y_A are the so-called Sudakov variables; in the collider system described in Sect. 3 the 4-vector $A_\perp$ has x and y components only:

$$A_\perp = (0, A_x, A_y, 0), \quad A_\perp^2 = -\mathbf{A}_\perp^2. \qquad (B.2)$$

In particular,

$$\begin{aligned} p_\pm &= x_\pm p_1 + y_\pm p_2 + p_{\pm\perp}, \\ \Delta &= x_\Delta p_1 + y_\Delta p_2 + \Delta_\perp, \\ q_i &= x_i p_1 + y_i p_2 + q_{i\perp}, \end{aligned} \qquad (B.3)$$

with $x_\pm$, $y_\pm$, $x = x_+ + x_-$ and $y = y_+ + y_-$ mentioned in (6).

In the used logarithmic approximation [see (20)] the decomposition of q_2 and r defined in (A.3) is simplified:

$$q_2 = y_2 p_2, \quad r = y_r p_2 + r_\perp, \qquad (B.4)$$
$$r^2 = -\mathbf{r}_\perp^2, \quad y_r = \frac{2}{x}\mathbf{r}_\perp \mathbf{k}_\perp,$$

with y_2 and $\mathbf{r}_\perp$ given in (22) and (25). Besides,

$$\begin{aligned} t - \mu^2 &= -2q_2 p_- = -s y_2 x_-, \\ u - \mu^2 &= -2q_2 p_+ = -s y_2 x_+, \\ t - u &= 2q_2 \Delta = s y_2 \xi x. \end{aligned}$$

Below we use the notation

$$e^{(a)} \equiv e_1^{(a)} = x^{(a)} p_1 + y^{(a)} p_2 + e_\perp^{(a)}, \qquad (B.5)$$

with

$$x^{(\pm)} = 0, \quad y^{(\pm)} = \frac{2\mathbf{e}_\perp^{(\pm)}\mathbf{k}_\perp}{sx},$$
$$y^{(0)} = \sqrt{-q_1^2}\,\frac{(2-x)}{xs}, \quad \mathbf{e}_\perp^{(0)} = \frac{\mathbf{k}_\perp}{\sqrt{-q_1^2}}. \qquad (B.6)$$

The normalization condition for the 4-vectors $e_\mu^{(a)}$ results in

$$\mathbf{e}_\perp^{(a)*}\mathbf{e}_\perp^{(b)} = \delta_{ab}, \quad a, b = \pm 1.$$

The following expressions will be useful ($i, j = x, y$):

$$\left(\mathbf{e}_\perp^{(+)*}\right)_i \left(\mathbf{e}_\perp^{(+)}\right)_j + \left(\mathbf{e}_\perp^{(-)*}\right)_i \left(\mathbf{e}_\perp^{(-)}\right)_j = \delta_{ij}, \qquad (B.7)$$

$$\left(\mathbf{e}_\perp^{(+)*}\right)_i \left(\mathbf{e}_\perp^{(-)}\right)_j + \left(\mathbf{e}_\perp^{(-)*}\right)_i \left(\mathbf{e}_\perp^{(+)}\right)_j = \delta_{ij} - 2e_i^{(x)} e_j^{(x)}, \qquad (B.8)$$

$$\left(\mathbf{e}_\perp^{(+)}\right)_i - \left(\mathbf{e}_\perp^{(-)}\right)_i = -\sqrt{2}e_i^{(x)}, \qquad (B.9)$$

where the vector $\mathbf{e}_\perp^{(x)}$ has the form [in accordance with definition (A.4)]

$$\mathbf{e}_\perp^{(x)} = \frac{\mathbf{r}_\perp}{|\mathbf{r}_\perp|}. \qquad (B.10)$$

B.2 Calculation of C_1^{ab}

Now we describe the calculation of trace (19) in the used approximation (20). First, we rewrite the trace C_1^{ab} with $a = 0, \pm 1$ and $b = \pm 1$ in the form of three terms

$$\begin{aligned} C_1^{ab} &= \frac{(-1)^{a+1}}{2} \times \\ &\times \mathrm{Tr}\left[\hat{p}_1' \hat{e}^{(a)*} \hat{p}_1 \left(\hat{e}^{(b)} \frac{\hat{p}_1 + \hat{q}_2}{s y_2} \hat{\Delta} - \hat{\Delta} \frac{\hat{p}_1' - \hat{q}_2}{s y_2 (1-x)} \hat{e}^{(b)}\right)\right] \\ &= \frac{(-1)^{1+a}}{2 s y_2 (1-x)} \left[N_1^{ab} + y_2\left(N_2^{ab} + N_3^{ab}\right)\right], \qquad (B.11) \\ N_1^{ab} &= \mathrm{Tr}\left[\hat{p}_1' \hat{e}^{(a)*} \hat{p}_1 \left((1-x)\hat{e}^{(b)} \hat{p}_1 \hat{\Delta} - \hat{\Delta} \hat{p}_1' \hat{e}^{(b)}\right)\right], \\ N_2^{ab} &= (1-x)\mathrm{Tr}\left[\hat{p}_1' \hat{e}^{(a)*} \hat{p}_1 \hat{e}^{(b)} \hat{p}_2 \hat{\Delta}\right], \\ N_3^{ab} &= \mathrm{Tr}\left[\hat{p}_1' \hat{e}^{(a)*} \hat{p}_1 \hat{\Delta} \hat{p}_2 \hat{e}^{(b)}\right]. \end{aligned}$$

The polarization 4-vector $e^{(a)}$ appears in C_1^{ab} in the combination $\hat{e}^{(a)*}\hat{p}_1$ only; therefore, the p_1 component of $e^{(a)}$ does not contribute ($\hat{p}_1\hat{p}_1 \approx 0$). Since $x^{(\pm)} = 0$, such a component is also absent in $e^{(b)}$. As a result, we can use all polarization 4-vectors in the form

$$e^{(a)} = y^{(a)} p_2 + e_\perp^{(a)}.$$

Next, for N_1 we use the relations

$$\hat{p}_1 \hat{e}^{(b)} \hat{p}_1 = s y^{(b)} \hat{p}_1,$$
$$\hat{p}_1' \hat{e}^{(b)} \hat{p}_1' = 2(e^{(b)} p_1')\hat{p}_1' = [(1-x) s y^{(b)} + 2(\mathbf{k}_\perp \mathbf{e}_\perp^{(b)})]\hat{p}_1',$$

which results in

$$N_1^{ab} = -2(\mathbf{k}_\perp \mathbf{e}_\perp^{(b)})\mathrm{Tr}\left[\hat{p}_1' \hat{e}^{(a)*} \hat{p}_1 \hat{\Delta}\right].$$

For the trace we obtain

$$\mathrm{Tr}\left[\hat{p}_1' \hat{e}^{(a)*} \hat{p}_1 \hat{\Delta}\right] = 2s\left[s(1-x) y^{(a)*} y_\Delta + \frac{-q_1^2}{s}(\mathbf{\Delta}_\perp \mathbf{e}_\perp^{(a)*}) + y_\Delta(\mathbf{k}_\perp \mathbf{e}_\perp^{(a)*}) + y^{(a)*}(\mathbf{\Delta}_\perp \mathbf{k}_\perp)\right].$$

The final result can be expressed in the form

$$N_1^{ab} = -4s\left[y_\Delta D_3 + \frac{-q_1^2}{s} D_2 + \left((1-x) y_\Delta + \frac{v}{s}\right) D_4\right],$$

where we have used the basic structures

$$\begin{aligned} D_0 &= (\mathbf{e}_\perp^{(a)*}\mathbf{e}_\perp^{(b)}), \quad D_1 = (\mathbf{e}_\perp^{(a)*}\mathbf{k}_\perp)(\mathbf{e}_\perp^{(b)}\mathbf{\Delta}_\perp), \\ D_2 &= (\mathbf{e}_\perp^{(a)*}\mathbf{\Delta}_\perp)(\mathbf{e}_\perp^{(b)}\mathbf{k}_\perp), \quad D_3 = (\mathbf{e}_\perp^{(a)*}\mathbf{k}_\perp)(\mathbf{e}_\perp^{(b)}\mathbf{k}_\perp), \\ D_4 &= s y^{(a)*}(\mathbf{e}_\perp^{(b)}\mathbf{k}_\perp), \quad D_5 = s y^{(a)*}(\mathbf{e}_\perp^{(b)}\mathbf{\Delta}_\perp). \end{aligned}$$

Similarly we obtain

$$\begin{aligned} N_2^{ab} &= 2s(1-x)\left[(v - q_1^2 x_\Delta) D_0 + D_1 - D_2 + x_\Delta D_4 + (1-x) D_5\right], \\ N_3^{ab} &= 2s\left[-v D_0 + D_1 + D_2 + (1-x) D_5\right], \end{aligned}$$

and the final expression for C_1^{ab}:

$$\begin{aligned} C_1^{ab} = \frac{(-1)^{1+a}}{y_2(1-x)} & \left[-xy_2(v-\xi \mathbf{k}_\perp^2)D_0 + (2-x)y_2 D_1 \right. \\ &+ \left(\frac{2q_1^2}{s} + xy_2 \right) D_2 - 2y_\Delta D_3 \\ &- \left(\frac{2v}{s} + 2(1-x)y_\Delta - y_2 x\xi(1-x) \right) D_4 \\ &\left. + \, y_2(1-x)(2-x)D_5 \right]. \end{aligned} \tag{B.12}$$

with

$$sxy_\Delta = 2x(p_1\Delta) = 2v - \xi(W^2 + \mathbf{k}_\perp^2).$$

B.3 Calculation of $T = \sum_{ab} M_{ab} C_1^{ab}$

Using (B.6) we find for T the expression

$$\begin{aligned} T &= (C_1^{++} + C_1^{-})M_{++} + (C_1^{+-} + C_1^{-+})M_{+-} \\ &+ (C_1^{0+} - C_1^{0-})M_{0+} \\ &= \frac{2}{y_2(1-x)}[G^0 M_{++} + G^2 M_{+-} + G^1 M_{0+}]. \end{aligned} \tag{B.13}$$

Taking into account (B.7), the basic structures related to the amplitude M_{++} are

$$D_0 = 2, \quad D_1 = D_2 = v, \quad D_3 = \mathbf{k}_\perp^2,$$
$$D_4 = \frac{2}{x}D_3, \quad D_5 = \frac{2}{x}D_1,$$

which leads to the coefficient G_0:

$$\begin{aligned} G^0 &= \frac{v}{x}\left[2(1-x)y_2 - \frac{(2-x)}{(1-x)}\frac{\mathbf{k}_\perp^2}{s} \right] \\ &+ \mathbf{k}_\perp^2 \left[y_2\xi - \frac{(2-x)y_\Delta}{x} \right]. \end{aligned} \tag{B.14}$$

Analogously we get for the basic structures related to M_{+-} [taking into account (B.8)]

$$D_0 = 0, \quad D_1 = D_2 = D_1^{(2)} = v - \frac{(v-\xi\mathbf{k}_\perp^2)(\mathbf{\Delta}_\perp^2 - \xi v)}{2\mathbf{r}_\perp^2},$$
$$D_3 = D_3^{(2)} = \mathbf{k}_\perp^2 - \frac{(v-\xi\mathbf{k}_\perp^2)^2}{2\mathbf{r}_\perp^2},$$
$$D_4 = \frac{2}{x}D_3^{(2)}, \quad D_5 = \frac{2}{x}D_1^{(2)},$$

which gives the coefficient G_2:

$$\begin{aligned} G^2 &= \left[\frac{2y_2}{x}\left(1 - x + \frac{x^2}{2} \right) - \frac{\mathbf{k}_\perp^2}{(1-x)s} \right] D_1^{(2)} \\ &+ \left[(1-x)y_2\xi - \frac{(2-x)y_\Delta}{x} - \frac{2v}{xs} \right] D_3^{(2)}. \end{aligned} \tag{B.15}$$

Finally, the coefficient G^1 is obtained from [using (B.9)]

$$D_0 = D_0^{(1)} = -\frac{v-\xi\mathbf{k}_\perp^2}{\sqrt{-2q_1^2\mathbf{r}_\perp^2}},$$
$$D_1 = D_1^{(1)} = -\frac{(\mathbf{\Delta}_\perp^2 - \xi v)\mathbf{k}_\perp^2}{\sqrt{-2q_1^2\mathbf{r}_\perp^2}},$$
$$D_2 = vD_0^{(1)}, \quad D_3 = \mathbf{k}_\perp^2 D_0^{(1)},$$
$$D_4 = \frac{2-x}{x(1-x)}\mathbf{k}_\perp^2 D_0^{(1)}, \quad D_5 = \frac{2-x}{x(1-x)}D_1^{(1)},$$

as follows:

$$\begin{aligned} G^1 &= -\mathbf{k}_\perp^2 \left[y_2\xi - \frac{2y_\Delta}{x} - \frac{2v}{x(1-x)s} \right] D_0^{(1)} \\ &- \frac{2-x}{x} y_2 D_1^{(1)}. \end{aligned} \tag{B.16}$$

The coefficients G^n depend on the vectors $\mathbf{\Delta}_\perp, \mathbf{k}_\perp$ and $\mathbf{r}_\perp$. Using the relation $\mathbf{\Delta}_\perp = 2\mathbf{r}_\perp + \xi\mathbf{k}_\perp$ [see (25)] and introducing the angle ϕ between the vectors $\mathbf{r}_\perp$ and $\mathbf{k}_\perp$ we get after some algebra the compact expression for T in the form of (28) and (29).

Appendix C
Some useful notes

C.1 Substitution rule for the contribution $\mathrm{d}\sigma_{13}$

Let us briefly describe the necessary changes for $\mathrm{d}\sigma_{13}$ in the case of electron–positron or electron–electron collisions:

$$e^-(p_1) + e^\pm(p_2) \to e^-(p_1') + e^\pm(p_2') + \pi^+\pi^-.$$

The contribution $\mathrm{d}\sigma_{13}$ has the form

$$\begin{aligned} \mathrm{d}\sigma_{13} &= 2\mathrm{Re}(\mathcal{M}_3^* \mathcal{M}_1)\frac{\mathrm{d}\Gamma}{2s} \\ &= -2\frac{(4\pi\alpha)^3}{q_1^2 q_2^2 k^2} \sum_{abc=\pm1,0} \mathrm{Re}\left(F_\pi^* M_{ab} \varrho_1^{ac} C_2^{bc} \right) \frac{\mathrm{d}\Gamma}{2s}, \end{aligned}$$

where ϱ_1^{ac} and C_2^{bc} are similar to ϱ_2^{bc} and C_1^{ac} in (18) and (19). $\mathrm{d}\sigma_{13}$ can be obtained from $\mathrm{d}\sigma_{12}$ under the exchange

$$p_1 \leftrightarrow p_2, p_1' \leftrightarrow p_2', q_1 \leftrightarrow q_2.$$

It is not difficult to check that in that case

$$\varrho_2^{bc} \to (-1)^{b+c}\varrho_1^{bc}, \quad C_1^{ac} \to \mp(-1)^{a+c}C_2^{ac}. \tag{C.1}$$

The sign $\mp$ in the last equation is in agreement with the transition from three e^- vertices in C_1^{ac} to three $e^\pm$ vertices in C_2^{ac}.

As a result, taking into account (A.7), we have

$$\mathrm{d}\sigma_{13} = \mp\mathrm{d}\sigma_{12}(p_1 \leftrightarrow p_2, p_1' \leftrightarrow p_2', q_1 \leftrightarrow q_2), \tag{C.2}$$

where the "minus" sign corresponds to electron–positron collisions considered here and "plus" to electron–electron collisions.

C.2 Absence of amplitude M_{+-} in $\mathrm{d}\sigma_{12}$ averaging over angle ϕ

The amplitude M_{+-} enters the result (24) with coefficient $C_1^{+-} + C_1^{-+}$ [see (B.13)]. Let us consider C_1^{-+} given by (B.11). Since

$$e^{(-)*} = -e^{(+)} \equiv -e$$

and

$$eq_1 = eq_2 = 0, \quad ep_1 = ep_1', \quad \hat{e}\hat{e} = 0,$$

we have

$$\hat{e}\hat{p}_1\hat{e} = \hat{e}\hat{p}_1'\hat{e} = 2(ep_1)\hat{e}.$$

Therefore, the C_1^{-+} coefficient can be simplified to a trace of four Dirac matrices making it easily calculable:

$$\begin{aligned} C_1^{-+} &= -(ep_1)\mathrm{Tr}\left\{\hat{e}\frac{\hat{p}_1+\hat{q}_2}{sy_2}\hat{\Delta}\hat{p}_1' - \hat{e}\hat{p}_1\hat{\Delta}\frac{\hat{p}_1-\hat{k}}{sy_2(1-x)}\right\} \\ &= \frac{(ep_1)^2 f_1 + (ep_1)(e\Delta)f_2}{sy_2(1-x)}, \end{aligned}$$

with

$$\begin{aligned} f_1 &= 8xp_1\Delta - 4(1-x)q_2\Delta, \\ f_2 &= 4xp_1k + 4(1-x)q_2(p_1+p_1'). \end{aligned}$$

It is easy to check that only two scalar products depend on the azimuthal angle ϕ:

$$\begin{aligned} 2ep_1 &= sy^{(+)} = \frac{2}{x}\mathbf{e}^{(+)}\mathbf{k}_\perp = -\frac{\sqrt{2}}{x}|\mathbf{k}_\perp|\mathrm{e}^{\mathrm{i}\phi}, \\ 2xp_1\Delta &= 4|\mathbf{r}_\perp||\mathbf{k}_\perp|\cos\phi - \xi\left(W^2 - \mathbf{k}_\perp^2\right). \end{aligned}$$

As a result, the structure of C_1^{-+} is

$$C_1^{-+} = (a + b\cos\phi)\mathrm{e}^{2\mathrm{i}\phi} + c\mathrm{e}^{\mathrm{i}\phi},$$

which leads to

$$\begin{aligned} C_1^{+-} + C_1^{-+} &= 2\mathrm{Re}C_1^{-+} \\ &= (b+2c)\cos\phi + 2a\cos 2\phi + b\cos 3\phi. \end{aligned}$$

Therefore, this coefficient disappears after averaging over ϕ:

$$\langle C_1^{+-} + C_1^{-+}\rangle_\phi = 0. \tag{C.3}$$

C.3 Low $k_\perp$ limit for $\mathrm{d}\sigma_{12}$

At small transverse momentum of the produced pion pair $k_\perp$, our result (24) and (28) is simplified to

$$\begin{aligned} \varepsilon_+\varepsilon_-\frac{\mathrm{d}\sigma_{12}}{\mathrm{d}^3p_+\mathrm{d}^3p_-} &= -\frac{\alpha^3}{4\pi^4}\frac{x}{W^6 d}\frac{\mathbf{k}_\perp\mathbf{\Delta}_\perp}{\mathbf{k}_\perp^2} \\ &\times\left(1 - y_2 + \frac{1}{2}y_2^2\right)L_2\Bigg[(1-x)\mathrm{Re}\left(F_\pi^* M_{++}\right) \\ &-\left(1 - x + \frac{1}{2}x^2\right)\mathrm{Re}\left(F_\pi^* M_{+-}\right)\Bigg], \end{aligned} \tag{C.4}$$

with $y_2 = W^2/(sx)$.

Analogously, in this limit the muon pair production [see (47)] takes the form

$$\begin{aligned} \varepsilon_+\varepsilon_-\frac{\mathrm{d}\sigma_{12}}{\mathrm{d}^3p_+\mathrm{d}^3p_-} &= \frac{4\alpha^3}{\pi^3}\frac{x}{W^6 d}\frac{\mathbf{k}_\perp\mathbf{\Delta}_\perp}{\mathbf{k}_\perp^2} \\ &\times\left(1 - y_2 + \frac{1}{2}y_2^2\right)L_2\Bigg[(1-x)\frac{4\mu^2}{W^2} \\ &-\left(1 - x + \frac{1}{2}x^2\right)\left(2 - \frac{\mathbf{\Delta}_\perp^2}{W^2}\right)\Bigg]. \end{aligned} \tag{C.5}$$

Both distributions are proportional to the transverse variable $v = \mathbf{k}_\perp\mathbf{\Delta}_\perp$ and do not depend on the longitudinal variable ξ. These results coincide with those of [3].

References

1. The second DAΦNE physics handbook, edited by L. Maiani, G. Pancheri, N. Paver (INFN, Frascati 1995)
2. International Workshop e^+e^- collisions from ϕ to J/Ψ (Novosibirsk, March 1–5, 1999)
3. V.L. Chernyak, V.G. Serbo, Nucl. Phys. B **67**, 464 (1973)
4. M. Diehl, T. Gousset, B. Pire, Phys. Rev. D **62**, 073014 (2000); M. Diehl, T. Gousset, B. Piret, O. Teryaev, Phys. Rev. Lett. **81**, 1782 (1998)
5. V. Savinov (CLEO), private communication
6. M. Galynsky, E.A. Kuraev, P.G. Ratcliffe, B.G. Shaikhatdenov, hep-ph/0003061
7. V.E. Balakin, V.M. Budnev, I.F. Ginzburg, Sov. ZhETF Pis'ma **11**, 559 (1970); V.M. Budnev, I.F. Ginzburg, Phys. Lett. B **37**, 310 (1971)
8. V.M. Budnev, I.F. Ginzburg, G.V. Meledin, V.G. Serbo, Phys. Rep. C **15**, 575 (1975)
9. G.L. Kotkin, V.G. Serbo, Yad. Fiz. **21**, 785 (1975)
10. E.A. Kuraev, L.N. Lipatov, N.P. Merenkov, M.I. Strikman, Yad. Fiz. **23**, 163 (1976)
11. V.N. Baier, V.S. Fadin, V.S. Khoze, E.A. Kuraev, Phys. Rep. **78**, 293 (1981)

Note added in proof: In connection with our discussion after (30), we were informed by M. Diehl that the corresponding expression in [4] was obtained without the requirement $-q_1^2 \gg W^2$.